

**NMR Spectroscopy**

# Systematic Evaluation of Polarizing Agents for Dynamic Nuclear Polarization Enhanced NMR

Ran Wei, Gilles Casano, Yuxuan Zhang, Ivanska M. Gierbolini-Colón, Yu Rao, Shubha S. Gunaga, Faith J. Scott, Jiaxin Zhou, Satyaki Chatterjee, Sanyog Kumari, Hakim Karoui, Mang Huang, Snorri Th. Sigurdsson, Gaël De Paëpe, Yangping Liu, Frédéric Mentink-Vigier, Amrit Venkatesh, Olivier Ouari, and Lyndon Emsley\*

**Abstract:** Dynamic nuclear polarization (DNP) can significantly enhance the sensitivity of nuclear magnetic resonance (NMR) spectroscopy, via the transfer of polarization from unpaired electrons to nuclei. As a result, there is considerable interest in improving DNP efficiency, particularly through the development of new polarizing agents (PAs). Here, a series of 32 PAs, including 26 dinitroxide and 6 hetero biradicals, of which 11 are introduced for the first time, were evaluated for their performance in DNP NMR experiments at magnetic field strengths of 9.4 T, 14.1 T, and 21.1 T. The PAs that are soluble in aqueous media were compared for different proton concentrations. A detailed comparison of the enhancement factors, polarization build-up times, contribution factors, and the resulting overall sensitivity factors is provided. We find that the class of narrow-line-broad-line biradicals not only yield the best performance at high field (21.1 T and 14.1 T) but remain among the best at intermediate fields (9.4 T). Specifically, SNAPol-1 and HyTEK2 are consistently among the best performing radicals at any field. Among the dinitroxides, notably at 9.4 T, the AsymPol-POK and M-TinyPol families stand out in proton-dense aqueous matrices, and a newly developed dinitroxide, NaphPolCbo, is found to provide the best overall sensitivity factor in organic solvent.

## Introduction

Solid-state nuclear magnetic resonance (NMR) spectroscopy can yield detailed atomic-level structural and dynamical information, leading to a broad range of applications in chemistry, biology, and medicine.<sup>[1]</sup> However, the inherently low sensitivity of NMR experiments is often a key bottleneck, and restricts its more widespread use. To alleviate this problem, over the last 20 years, dynamic nuclear polarization (DNP) has emerged as an efficient method to dramatically enhance the sensitivity of NMR experiments, via the transfer of the larger Boltzmann polarization of unpaired electron spins to

nearby nuclear spins.<sup>[2–5]</sup> The spectacular progress in this field has been enabled by many developments including new hardware, such as new microwave sources, fast spinning probes, and very low temperatures, and the introduction of novel polarization agents and sample formulation strategies.<sup>[6]</sup> Today, DNP in solid-state magic angle spinning (MAS) NMR typically provides very significant sensitivity enhancement,<sup>[7]</sup> which has successfully facilitated applications of solid-state NMR to nanoparticles,<sup>[8–14]</sup> catalysts,<sup>[15–22]</sup> battery materials,<sup>[23–26]</sup> photovoltaics,<sup>[27]</sup> building materials,<sup>[28–31]</sup> nucleic acid arrays,<sup>[32]</sup> proteins,<sup>[33–39]</sup> saccharides,<sup>[40–47]</sup> cells,<sup>[48–59]</sup> and complex drug formulations.<sup>[60–68]</sup>

[\*] R. Wei, Y. Zhang, Y. Rao, L. Emsley  
 Institut des Sciences et Ingénierie Chimiques, École Polytechnique  
 Fédérale de Lausanne (EPFL), Lausanne CH-1015, Switzerland  
 E-mail: [lyndon.emsley@epfl.ch](mailto:lyndon.emsley@epfl.ch)

G. Casano, H. Karoui, O. Ouari  
 Aix-Marseille Univ., CNRS, Institut de Chimie Radicalaire UMR 7273,  
 Marseille 13013, France

I. M. Gierbolini-Colón, S. S. Gunaga, F. J. Scott, F. Mentink-Vigier,  
 A. Venkatesh  
 National High Magnetic Field Laboratory, Florida State University,  
 Tallahassee, FL 32301, USA

J. Zhou, M. Huang, Y. Liu  
 Tianjin Key Laboratory on Technologies Enabling Development of  
 Clinical Therapeutics and Diagnostics, School of Pharmacy, Tianjin  
 Medical University, Tianjin 300070, P.R. China

S. Chatterjee, S. Kumari, S. T. Sigurdsson  
 Department of Chemistry, University of Iceland, Science Institute,  
 Reykjavik 107, Iceland

G. De Paëpe  
 Univ. Grenoble Alpes, CEA, IRIG-MEM, Grenoble 38000, France

G. De Paëpe  
 INAC-MEM, Grenoble F-38000, France

F. Mentink-Vigier  
 Department of Chemistry and Biochemistry, Florida State University,  
 Tallahassee, FL 32306, USA

 Additional supporting information can be found online in the Supporting Information section

 © 2025 The Author(s). Angewandte Chemie International Edition published by Wiley-VCH GmbH. This is an open access article under the terms of the [Creative Commons Attribution](https://creativecommons.org/licenses/by/4.0/) License, which permits use, distribution and reproduction in any medium, provided the original work is properly cited.

Standard high-resolution solid-state MAS DNP experiments typically involve the introduction of polarizing agents (PAs) containing unpaired electrons to the sample of interest. In MAS DNP, the polarization is transferred from electron spins to nearby nuclear spins upon continuous-wave microwave irradiation at cryogenic temperatures ( $\sim 100$  K),<sup>[69–73]</sup> followed by spin diffusion into the bulk of the sample.<sup>[74–79]</sup> (We note that lower temperatures are also accessible.<sup>[80–83]</sup>) The efficiency of this process depends on multiple factors, notably the complex nature of the PAs hosting the unpaired electrons. For example, cross effect (CE) DNP using biradicals is the most efficient mechanism at typical NMR fields, embodied for example in dinitroxide biradicals.<sup>[6,84,85]</sup> The last two decades have therefore seen efforts geared towards understanding the factors that determine the DNP efficiency and improving biradical PAs. Since the first example of using a dinitroxide PA for CE MAS DNP in 2004,<sup>[84]</sup> a series of design principles have been identified to contribute to the DNP efficiency, such as the optimal relative orientation of the electron  $g$ -tensors (which has been referred to as the distance between the  $g$ -tensors),<sup>[86–88]</sup> increased electron spin relaxation times leading to better saturation factors,<sup>[89–91]</sup> optimizing the magnitude of electron-electron spin couplings,<sup>[76,92–100]</sup> optimal conformational properties around the nitroxide,<sup>[101,102]</sup> and favorable polarization transport pathways.<sup>[103–105]</sup> This has collectively resulted in improved polarizing agents for aqueous-based and organic solvents [specifically 1,1,2,2-tetrachloroethane (TCE)],<sup>[106]</sup> at 9.4 T and  $\sim 100$  K. In parallel, design principles have been improved through the awareness that the overall sensitivity is influenced not only by the enhancement factors but also by build-up times, paramagnetic quenching, and depolarization effects.<sup>[45,76,91,107–113]</sup>

On the other hand, the advent of higher field DNP instrumentation (e.g.,  $\geq 18.8$  T) triggered the quest for polarizing agents tailored for high fields. The principal challenge at higher fields is that for dinitroxide radicals that perform well at 9.4 T, the CE efficiency usually suffers from a decrease at higher field. To alleviate this last problem, one strategy is to increase the magnitude of electron-electron (e-e) magnetic interactions, that is, the dipolar interaction ( $D$ ) and exchange interaction ( $J$ ), of a PA.<sup>[98,114]</sup> For example, dinitroxide PAs such as the AsymPol<sup>[93,102,115]</sup> and TinyPol<sup>[97,116]</sup> families were designed to adopt relatively shorter linkers, hence stronger e-e interactions, while maintaining the other favorable design features.<sup>[88,117,118]</sup> The AsymPol radicals utilize a short carboxamide tether that yielded larger dipolar ( $D \approx 56$  MHz) and exchange couplings ( $J \approx 100$  and  $J \approx 120$  MHz).<sup>[93,115]</sup> The increased e-e couplings also directly contribute to short polarization build-up times and reduced depolarization loss for the AsymPol radicals, where strong  $J$  couplings are also predicted to attenuate the MAS-induced depolarization effect by increasing the probability of adiabatic electron-electron crossings.<sup>[93,109,111]</sup> Similarly, the distance between the two electrons in TinyPol was estimated from molecular dynamics simulations to be distributed around ca. 10.4 Å, in comparison to around 11.6 Å in AMUPol, that led to a predicted increase in the average dipolar coupling from 33 MHz for AMUPol (corresponding well to the measured values of 35–

36 MHz)<sup>[119,120]</sup> to a prediction of 47 MHz for TinyPol, and a change in their respective exchange interaction from  $J \sim 42$  MHz<sup>[121]</sup> to a  $J$  distribution of  $\sim 5$ , 24, and 110 MHz with a 23%, 47%, and 30% weight each.<sup>[97]</sup> The TinyPol structure yielded an improvement of enhancement from 50 (AMUPol) to 90 (M-TinyPol) at 18.8 T, 40 kHz MAS.<sup>[97]</sup>

An alternative strategy to address microwave power limitation<sup>[98,99]</sup> while providing faster buildup times<sup>[76]</sup> at high fields is the development of so-called hetero-biradicals, a class of polarizing agents that chemically tether a narrow-line radical [e.g., BDPA (1,3-bisdiphenylene-2-phenylallyl) or trityl] with a broad-line radical (e.g., nitroxide). The narrower line enables both a more efficient microwave saturation and better polarization transfer (slower microwave and CE rotor events)<sup>[98,99]</sup> and often have longer relaxation times.<sup>[122]</sup> Following the development of the TEMTriPol series in 2015 by Griffin and co-workers,<sup>[92]</sup> other trityl-nitroxide hetero PAs have been introduced, such as NATriPol,<sup>[123]</sup> SNAPol,<sup>[124]</sup> STAPol,<sup>[125]</sup> PyrroTriPol<sup>[126]</sup>; and the BDPA-nitroxide hetero PA, HyTEK,<sup>[94]</sup> designed for high field DNP, and capable of yielding enhancements  $>100$  at magnetic field of 18.8 T.<sup>[94,124–126]</sup> During this endeavor, hetero PAs were found to benefit from additional advantages, such as a reduced depolarization effect observed for the hetero PAs when modest concentration are employed. This depolarization effect of CE DNP accounts for the depleted nuclear Boltzmann equilibrium polarization induced by the presence of paramagnetic PAs under MAS, in the absence of microwave irradiation.<sup>[109,111]</sup> TEMTriPol-1, for example, showed a negligible depolarization effect.<sup>[88,112]</sup>

Overall, the aforementioned two classes of radicals—dinitroxide biradicals and narrow-line broad-line biradicals—constitute the currently most studied radicals in the development of PAs for CE MAS DNP today, leading to a vast, diverse collection of biradical polarizing agents.

While the focus of the PA development was historically upon the DNP enhancement factor ( $\epsilon$ ), it is now well-accepted that  $\epsilon$  does not capture the overall DNP performance. Additional parameters such as the build-up time of the polarization ( $T_B$ ), which relates to how fast experiments are repeated, and the signal quenching/depolarization, due to the presence of the paramagnetic radical, also need to be included.<sup>[45,76,91,107–113]</sup> An alternate way to measure sensitivity could be to evaluate the SNR/sqrt(time)/mg,<sup>[45,93,126]</sup> However, due to the numerous samples, measuring SNR systematically across different experimental sessions and instruments was challenging for such a large series (see SI). Instead, we recently evaluated the *overall sensitivity factors* ( $S$ ) provided by a series of eighteen dinitroxide PAs at 9.4 T and 100 K,<sup>[7]</sup> where the three key parameters—the  $^1\text{H}$  DNP enhancement factor ( $\epsilon_H$ ), the build-up time of the polarization ( $T_B$ ), and the contribution factor ( $\theta = \epsilon_{\text{depo}} \times \theta_q$ ), which includes both depolarization  $\epsilon_{\text{depo}}$  and quenching ( $\theta_q$ )—were systematically measured to yield the overall DNP performance of a PA, following Equation (1).<sup>[7]</sup>

$$S = \epsilon_H \times \theta \times T_B^{-1/2} \quad (1)$$

Notably, it is important to include both the enhancement factor and the contribution factor, since the objective is to compare the signal that is obtained with DNP to that which would be obtained from an “ordinary” NMR sample that would not contain the polarizing agent. For that it is necessary to compound the gain seen through the enhancement factor measured on the DNP sample, with the overall loss of signal due to the presence of the paramagnetic PA.<sup>[107,113]</sup>

The main motivation for that work<sup>[7]</sup> stemmed from the fact that despite the extensive reports of polarizing agents for DNP, it had been difficult to directly compare the relative performance of the PAs available today from the literatures. Furthermore, the performance is also affected by miscellaneous factors such as the spinning rate,<sup>[127]</sup> the strength of the microwave irradiation (e.g., rotor diameter,<sup>[100,127]</sup> rotor material,<sup>[71]</sup> or source of the radiation), the experimental protocol (e.g., degassing<sup>[128]</sup> or temperature), presence of solutes, etc. Different research groups often report radical performance under slightly different conditions. Therefore, here we attempted a global assessment conducted under systematically controlled conditions allows to establish guidelines for the choice of optimal PAs today, and for further PA optimization in the future. In particular, the past comparison at 9.4 T in organic and deuterated aqueous media unexpectedly revealed that a large group of dinitroxides all yielded very similar overall performance, due to the three factors compensating for each other, and highlighting the existence of a “glass ceiling” in current performance.<sup>[7]</sup>

In this light, here, we extend the approach to a systematic evaluation of a collection of 32 state-of-the-art polarizing agents, consisting of 26 dinitroxide biradicals and 6 hetero biradicals, among which 11 PAs are newly-developed. Here, our initial focus was to evaluate performance of PAs at high magnetic fields, and the comparison is performed at field strengths ranging from 21.1, 14.1, to 9.4 T. The reader should keep in mind that the present comparison is done in identical 3.2 mm rotors that may not be optimal for very high field DNP,<sup>[127]</sup> but the intention was to be systematic. Notably, this is the first time that the two classes of biradicals are simultaneously compared at these fields, and in solvent systems with different proton concentrations (see below). We find that at 21.1 T and 100 K, hetero biradicals far outperform the dinitroxides, with SNAPol-1 and HyTEK2 being the best candidates in aqueous and organic solvents, respectively. However, we also find, that at both 14.1 and 9.4 T, SNAPol-1 and HyTEK2 remain among the best PAs, mostly owing to their high contribution factors. Among the dinitroxide biradicals, at 9.4 T, NaphPolCbo yields the highest overall sensitivity factor in the organic solvent, and we find that the AsymPol-POKs, and the M-TinyPol series provide excellent performance, particularly in proton-dense aqueous solvents.

## Results and Discussion

### State-of-the-art Polarizing Agents

Figure 1 shows the chemical structures of the polarizing agents studied in this work. The PAs are categorized based on

their solubility in organic (Figure 1a) and aqueous solvents (Figure 1b) respectively. Three glass-forming matrices were utilized, including 1,1,2,2-tetrachloroethane (TCE),<sup>[106]</sup> classic partially deuterated  $d_8$ -glycerol: $D_2O:H_2O$  (v:v:v 6:3:1),<sup>[129,130]</sup> and fully protonated glycerol: $H_2O$  (v:v 6:4).<sup>[131]</sup> The latter two formulations are hereafter referred to as deuterated glycerol/water and protonated glycerol/water, with  $^1H$  concentrations of 11 and 110 M, respectively. The protonated glycerol/water solvent was included to investigate the impact of proton density on the DNP performance of PAs, since it has been shown to impact the polarization dynamics and is highly relevant for applications in proton-rich environments such as organic and biomolecular systems.<sup>[75,79,102,103,115,116,132]</sup> All PAs in TCE were studied at 16 mM radical concentration. PAs in the two glycerol/water solvents were studied at 8–16 mM depending on their solubility. Quantitative EPR experiments were performed to estimate the final radical concentrations in the solutions (see Table S9).

Note that from an experimental point of view, it is challenging to have identical experimental conditions across all samples. Errors can stem from differences in concentrations, in measuring sample masses, in sample temperature, in glass formation, radical purity, or other sources. It is not feasible to make the tens of separate samples and measurements for each radical that would be needed to rigorously assess errors. Instead, here, we have attempted to reduce errors using systematic best practices, with the same operators and procedures on the same spectrometers, and we present these results with an estimation for the overall error. The systematic errors, can affect all three key parameters (polarization buildup times, contribution factors, and enhancements), and can in turn impact the details of the rankings found below, and they are accounted for through the reported uncertainties, but we believe the trends we report are reliable. Details of the sample preparation and DNP NMR experiments are given in the SI.

The PAs evaluated in this work were selected based on the best-performing candidates reported in a large selection of literature.<sup>[7,90,92–94,97,102,103,115,116,124–126,133]</sup> In addition to this, 11 newly synthesized PAs are introduced here for the first time (Figure 1, red-labels).

Regarding the design of the new radicals, the bCTolCbo, NaphPolCbo, HyPolCbo, HydroPolCbo, PyPolPEG2Cbm, HydroCbm dinitroxide PAs are designed based upon a previous study where carbonate and carbamate linkers yielded shorter  $T_B$  and larger  $J$  couplings as compared to their counterparts with a urea linker or a bis-spiroketal linker, thereby yielding advantageous overall performance.<sup>[7]</sup> For example, in our previous studies conducted at 9.4 T, TEKPolCbo ( $S = 40 s^{-1/2}$ ) showed a moderate improvement in the overall performance as compared to TEKPol ( $S = 38 s^{-1/2}$ ),<sup>[7]</sup> while NaphPol ( $S = 50 s^{-1/2}$ ) improved the overall sensitivity factor when replacing the phenyl groups of TEKPol with naphthyl groups to improve the  $^1H$ - $^1H$  polarization transfer.<sup>[103]</sup> (Note that in the above sentence and the following discussion, for clarity of the text, we only report the measured value of  $S$ , without errors. All the errors are shown in the figures and reported in the Tables in SI). Taken together, the development of NaphPolCbo is

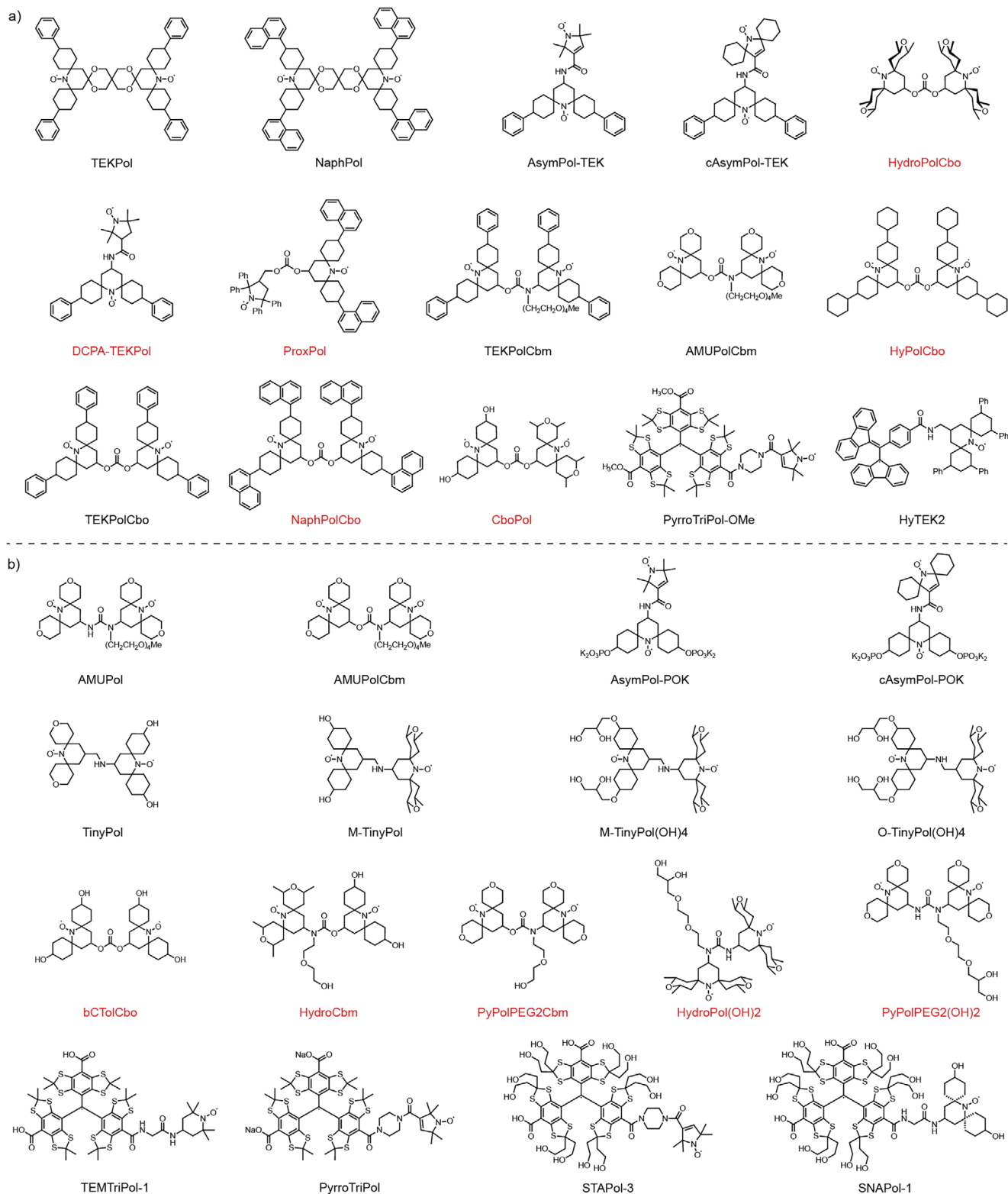


**Figure 1.** Chemical structures of the state-of-the-art polarizing agents evaluated in this work for a) 1,1,2-tetrachloroethane (TCE), and b) deuterated glycerol/water ( $d_8$ -glycerol:D<sub>2</sub>O:H<sub>2</sub>O, v:v:v 6:3:1) and protonated glycerol/water (glycerol:H<sub>2</sub>O, v:v 6:4), respectively. The newly designed radicals are indicated in red, while previously reported radicals are in black. Details for the synthesis of the new radicals are provided in the supporting information.

therefore straightforward, and as discussed below yielded here the highest overall sensitivity gain ( $S = 55 \text{ s}^{-1/2}$ ) at 9.4 T in TCE among the dinitroxide PAs. Then, the design principles used for the recently published M-TinyPol(OH)4 and O-TinyPol(OH)4, are used to introduce HydroPol(OH)2, PyPolPEG2(OH)2 here, with additional dihydroxyl antenna chains to improve the hydrophilicity as well as to increase the molecular weight, which have both been proved to be beneficial for DNP enhancement.<sup>[90,116,121,124]</sup> As we see below, in deuterated glycerol/water, the improved water solubility of M-TinyPol(OH)4 ( $S = 72 \text{ s}^{-1/2}$ ) immediately results in a 26% improvement in the overall sensitivity factor as compared to TinyPol ( $S = 57 \text{ s}^{-1/2}$ ).

### DNP Performance at 21.1 T

The measured values of the three key parameters— $^1\text{H}$  DNP enhancement ( $\varepsilon_{\text{H}}$ ), polarization build-up time ( $T_{\text{B}}$ ), contribution factor ( $\theta$ )—of all the PAs in TCE, deuterated and protonated glycerol/water at 21.1 T and 100 K are shown in Figure 2. The resultant overall sensitivity factor ( $S$ ) provided by all PAs is then shown in Figure 3.

We immediately note the unparalleled performance provided by the class of hetero PAs at 21.1 T, with all the hetero PAs leading the overall sensitivity factor in the three different solvent systems. In TCE, HyTEK2 and PyrroTriPol-OMe outperform all the dinitroxide biradicals. Notably, HyTEK2 ( $S = 19 \text{ s}^{-1/2}$ ) provides a factor 2.6 improvement in overall sensitivity factor relative to PyrroTriPol-OMe ( $S = 7 \text{ s}^{-1/2}$ ), and a factor 5.6 as compared to the best-performing dinitroxides cAsymPol-TEK and NaphPolCbo ( $S = 3 \text{ s}^{-1/2}$ ). HyTEK2 consists of a narrow-line BDPA moiety and a broad-line nitroxide tethered by a methylene carboxamide linker. HyTEK2 was designed by optimizing the e-e interactions via the linker length, and by lengthening the electron relaxation time of the nitroxide unit by functionalization with bulky 4-phenyl spirocyclohexyl groups.<sup>[94]</sup> Similarly, PyrroTriPol-OMe was designed with a piperazine linker connecting a trityl and a five-membered ring nitroxide (Figure 1). The good performance observed for HyTEK2 may be the sign that longer relaxation times offered by BDPA, appear to favor higher enhancement and it also confirms that somewhat flexible linkers are not necessarily a major obstacle to obtaining good DNP efficiency in narrow-line broad-line biradicals. Indeed, while the flexibility can affect unfavorably the e-e couplings, hetero PAs are less sensitive to the relative orientation of the  $g$ -tensors than dinitroxides thus still yielding good DNP performance.<sup>[88]</sup> Finally, despite the relative underperformance of dinitroxide PAs at 21.1 T, it is worth noting that all the ranking appears to group dinitroxides in two categories: those with relatively short linkers (amide, carbonate, carbamate) exhibiting overall better performance compared to those with rigid spiroketal linkers, again in line with previous analysis and the design strategies used to develop for high-fields, where stronger e-e interactions are important.<sup>[76,92–100]</sup>

Similar trends are observed for the hetero PAs in aqueous solvents shown in Figure 3. Specifically, in deuterated gly-

cerol/water, SNAPol-1 ( $S = 31 \text{ s}^{-1/2}$ ) is the best performing, yielding a 60% improvement in  $S$  over the runner-up, STAPol-3 ( $S = 20 \text{ s}^{-1/2}$ ), and a factor 2 improvement over TEMTriPol-1 ( $S = 15 \text{ s}^{-1/2}$ ) and PyrroTriPol ( $S = 12 \text{ s}^{-1/2}$ ). The superior performance of SNAPol-1 is primarily ascribed to two factors,<sup>[124]</sup> i) its high hydrophilicity introduced notably by fourteen hydroxyl groups, and ii), as compared to STAPol-3, TEMTriPol-1 and PyrroTriPol, in SNAPol-1 the replacement of the methyl groups on one or both moieties with bulkier spirocyclohexanol groups was claimed to increase the electron relaxation times,<sup>[89,90]</sup> thereby increasing the saturation factor and leading to an improved DNP enhancement factor of  $\varepsilon_{\text{H}} = 98$  compared to STAPol-3 ( $\varepsilon_{\text{H}} = 74$ ), TEMTriPol-1 ( $\varepsilon_{\text{H}} = 34$ ), and PyrroTriPol ( $\varepsilon_{\text{H}} = 32$ ). We note that previous reports have signaled that TEMTriPol and PyrroTriPol radicals suffer from a tendency to aggregate in aqueous solvents which is detrimental to DNP performance.<sup>[123,125,126,134]</sup> The results observed here confirms previous reports, and highlight again, from the synthetic perspective, on the importance of solubility to DNP performance. A radical concentration of 10 mM was used for four of the hetero PAs in the comparison (instead of 16 mM), due to the limited solubility of TEMTriPol-1 and PyrroTriPol. However, SNAPol-1 does not suffer from limited solubility, and increasing the radical concentration from 10 to 15 mM was previously shown to improve the overall DNP efficiency further by  $\sim 8\%$ .<sup>[124]</sup>

A key advantage of hetero PAs is clearly reflected by their high contribution factors (Figure 2). Apart from STAPol-3 which has a contribution factor of 0.6, all the other trityl-nitroxide PAs yielded a high contribution factor of ca. 0.8, owing to the design principle of tethering a broad line and a narrow line radical, limiting depolarization effect through reverse CE, compared to most dinitroxides.<sup>[112,126]</sup> This reduced depolarization effect contributes significantly to their good overall performance, and is maintained for hetero PAs across the magnetic fields studied in this work. Clearly, at 21.1 T, the dinitroxide radicals are outperformed by the hetero PAs in 3.2 mm rotors. A large ensemble of the dinitroxides yield very similar overall sensitivity factors, with the M/O-TinyPol(OH)4 and cAsymPol-POK appearing moderately better. This is not surprising since both were designed to have shorter linkers, with larger electron-electron interactions, to mitigate the reduction in enhancement at higher fields and maintain fast buildup times.

The right-hand panel in Figure 3 compares the relative performance of selected water-soluble PAs in protonated glycerol/water. For such media, SNAPol-1 remains the most efficient PA in this environment, outperforming the other candidates. An overall sensitivity factor  $S$  of  $21 \text{ s}^{-1/2}$  was obtained for SNAPol-1, 2.6 times higher than that of PyrroTriPol ( $S = 8 \text{ s}^{-1/2}$ ). Notably, the high  $^1\text{H}$  concentration (110 M) of protonated glycerol/water means that 10 times more  $^1\text{H}$  nuclei need to be polarized per radical (for the same radical concentration), as compared to the deuterated glycerol/water matrix. This leads to a systematic decrease in the overall sensitivity factor across nearly all the PAs evaluated, see Figure 4a, but one should note that the total signal intensity in the protonated samples is in general higher. It is also interesting to note that among the dinitroxide

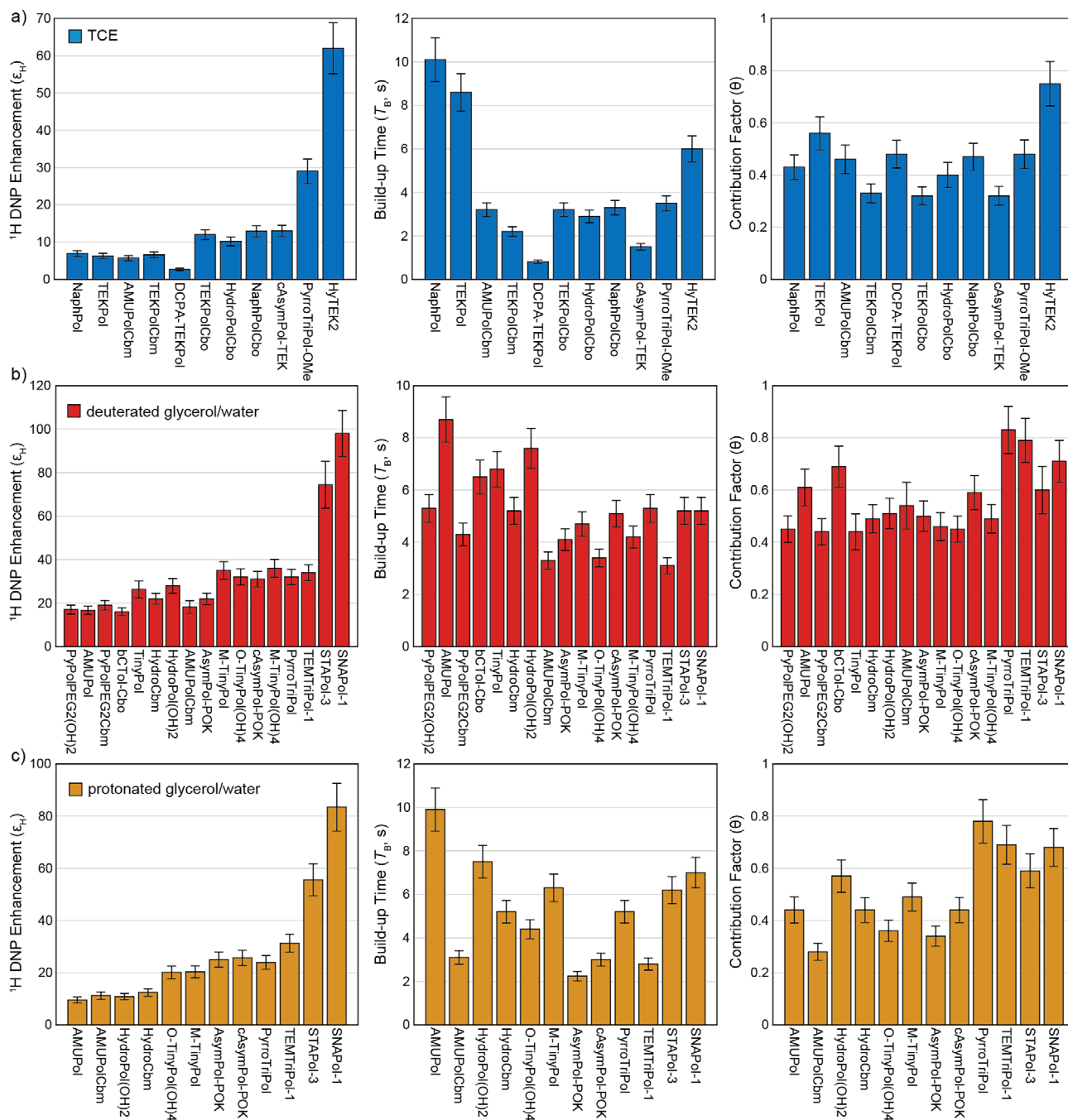


**Figure 2.** Comparison of the measured values of the three key parameters,  $^1\text{H}$  DNP enhancement factor ( $\epsilon_H$ ), build-up time ( $T_B$ ), and contribution factor ( $\theta$ ) of polarizing agents in a) TCE, b) deuterated glycerol/water, and c) protonated glycerol/water respectively, measured at 21.1 T, 100 K, and 8 kHz MAS. The values and the error analysis are detailed in the SI.

biradicals, the AsymPols clearly stand out despite the limited microwave field amplitudes available in the 3.2 mm rotor at 21.1 T.

A detailed comparison of the three key parameters between the two matrices is shown in Figure S5. From deuterated glycerol/water to protonated glycerol/water, the  $S$  provided by SNAPol-1 and PyrrroTriPol decreased by 30%, while most dinitroxide-based PAs decrease by around 50%. Despite the fact that at 21.1 T, all the dinitroxide PAs yield overall sensitivity factors that are far below SNAPol-

1; interestingly, the two AsymPol-POKs are the only ones to maintain good performance as compared to other PAs in proton-dense matrix, and decrease by only 20% for cAsymPol-POK, and even slightly increased to +5% for AsymPol-POK (Figure 4a). The ability of the AsymPol-POKs to polarize proton-dense matrix is reflected in the comparison of their build-up times shown in Figure S5d. In contrast to other PAs the  $T_B$  of both AsymPol-POKs is shorter in the protonated matrix. This trend is maintained at other field strengths, as discussed below, in line with the

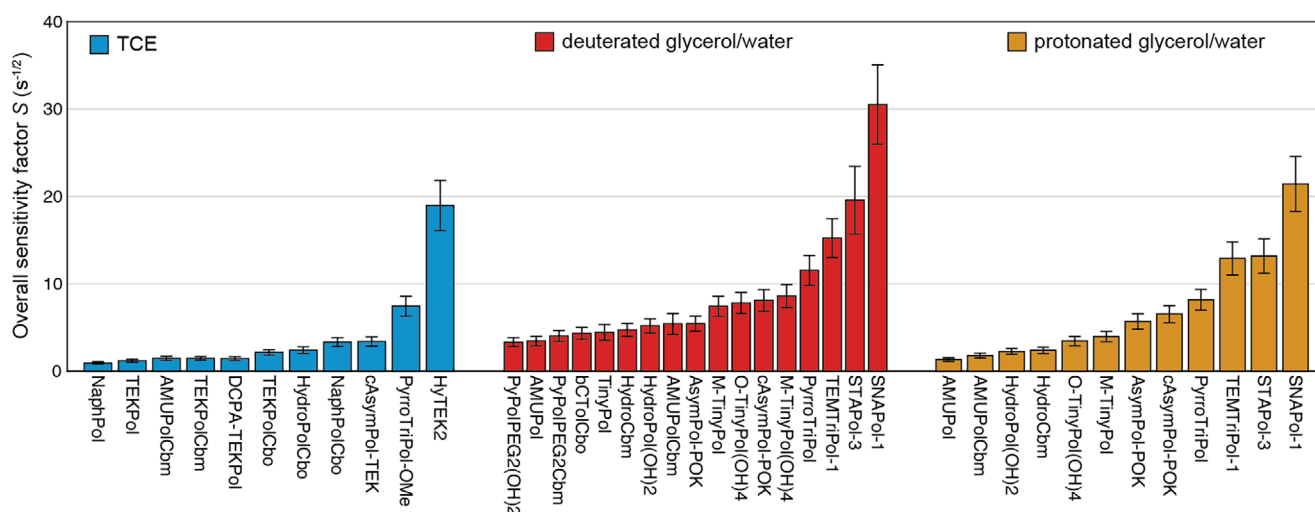


**Figure 3.** The overall sensitivity factor ( $S$ ) provided by polarizing agents in TCE, deuterated glycerol/water and protonated glycerol/water respectively, measured at 21.1 T, 100 K, 8 kHz MAS. The values and the error analysis are detailed in the SI.

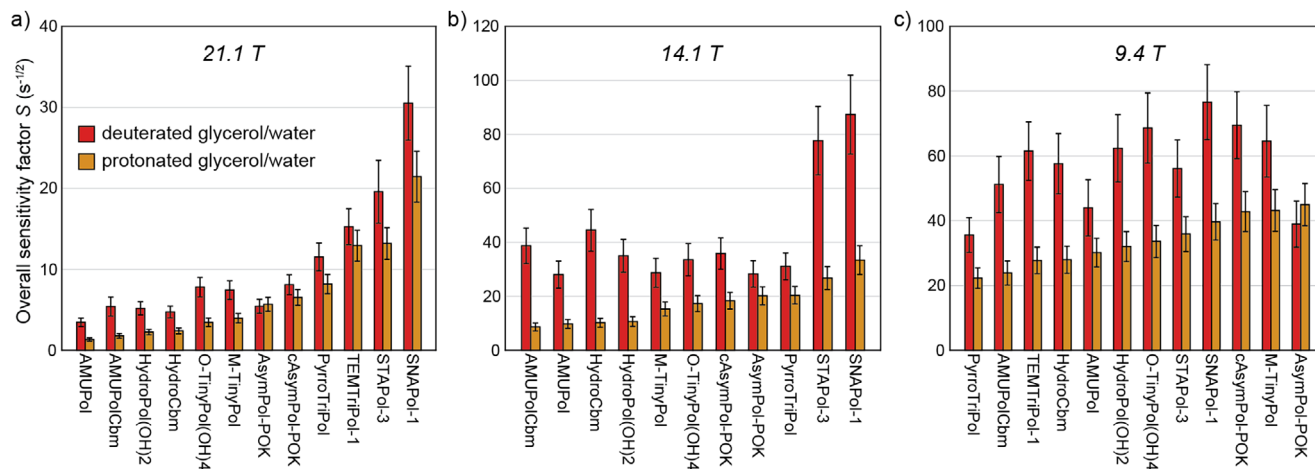


**Figure 4.** The comparison of overall sensitivity factor ( $S$ ) provided by polarizing agents in deuterated glycerol/water and protonated glycerol/water, at different magnetic field strengths of a) 21.1 T, b) 14.1 T, and c) 9.4 T, at 100 K and 8 kHz MAS. The values and the error analysis are detailed in the SI.

original report.<sup>[115]</sup> Recently it has been shown that AsymPols can efficiently directly hyperpolarize the protons located in the nearby solvent, which would be an advantage in fully protonated media.<sup>[104,105,115]</sup> Conversely, other biradicals have been shown to distribute hyperpolarization efficiently through protonated antenna groups on the radical scaffolds.<sup>[103,116]</sup>

Overall, the hetero PAs are remarkably more efficient at 21.1 T than the dinitroxide PAs, in all the solvent systems studied here. BDPA-TEMPO hetero biradicals were introduced as early as 2009 where the two moieties were directly tethered by an amide bond.<sup>[135]</sup> No DNP measurements were made, although now it appears clear that the short amide linker would introduce a too large e-e interaction to be efficient.<sup>[92,94]</sup> Later, synthetic routes for water-soluble BDPA derivatives were proposed, through functionalizing via the addition of carboxylic acid,<sup>[136]</sup> sulphonate groups,<sup>[137]</sup> or the tetraalkyl/aryl-ammonium groups,<sup>[138]</sup> all of which can potentially serve as the precursor of water-soluble BDPA-

nitroxide hetero biradicals. Interestingly, SA-BDPA showed both a higher solid-effect enhancement and a narrower linewidth as compared to trityl.<sup>[137]</sup> In 2020, a tetraalkyl/aryl-ammonium BDPA derivative was tethered to TEMPO via an amide linker.<sup>[138]</sup> The DNP efficiency of this hetero PA was again not measured and is most likely to perform poorly due to the short linker, as was observed for TEMTriPol-0 and ProxTriPol.<sup>[92]</sup> These efforts to explore new synthetic routes to water-soluble BDPA based hetero radicals for high-field DNP open up interesting new pathways that look all the more relevant given the results presented here for HyTEK2 in organic solvent. On the other hand, in 2007, a mixture of trityl and nitroxide radicals was reported to provide favorable DNP enhancements.<sup>[139]</sup> Then, the first trityl-nitroxide class of hetero biradicals was developed in 2013.<sup>[140]</sup> Although no DNP experiments were conducted, this work highlighted the tunability of magnetic properties by adjusting the chemical linker and this was later experimentally verified by DNP.<sup>[92]</sup>

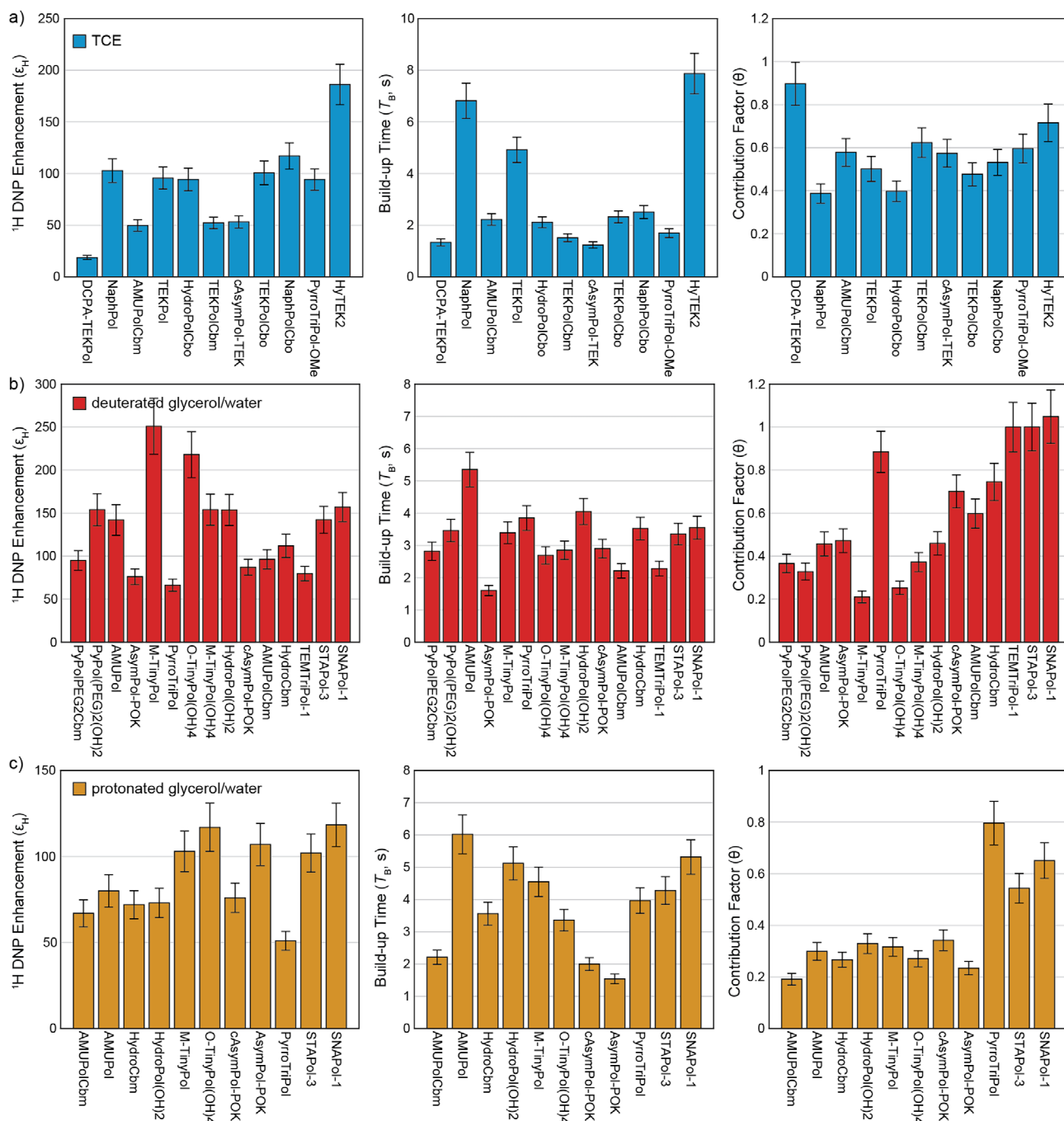


**Figure 5.** Comparison of the measured values of the three key parameters,  $^1\text{H}$  DNP enhancement factor  $\epsilon_{\text{H}}$ , build-up time  $T_{\text{B}}$ , and contribution factor  $\theta$  of polarizing agents in a) TCE (with h-BN), b) deuterated glycerol/water, and c) protonated glycerol/water respectively, measured at 14.1 T, 100 K, and 8 kHz MAS. The values and the error analysis are detailed in the SI.

Other trityl-nitroxide hetero PAs for organic solvents were also introduced, and evaluated only at 9.4 T yielding modest DNP enhancements of ca. 50<sup>[141]</sup> and 30.<sup>[142]</sup> We note that very recently, a verdazyl-nitroxide biradical was developed, termed VerTEKOL that yields improved enhancement factors in TCE at 600 MHz.<sup>[143]</sup> Now given the superior performance highlighted here for the hetero PAs in both aqueous and organic solvents, there is no doubt room to develop other hetero PAs with improved DNP efficiency at high fields.

### DNP Performance at 14.1 T

With the evaluation above at 21.1 T, the next step is to extend the measurements to fields of 14.1 and 9.4 T. As stated above, since the hetero PAs were initially designed for high-field applications, previous focus has been primarily upon their performance at fields  $\geq 18.8$  T. Additionally, considerable efforts to achieve optimal PA efficiency at 9.4 T have largely been focused towards the development of dinitroxide biradicals, which are chemically stable under many

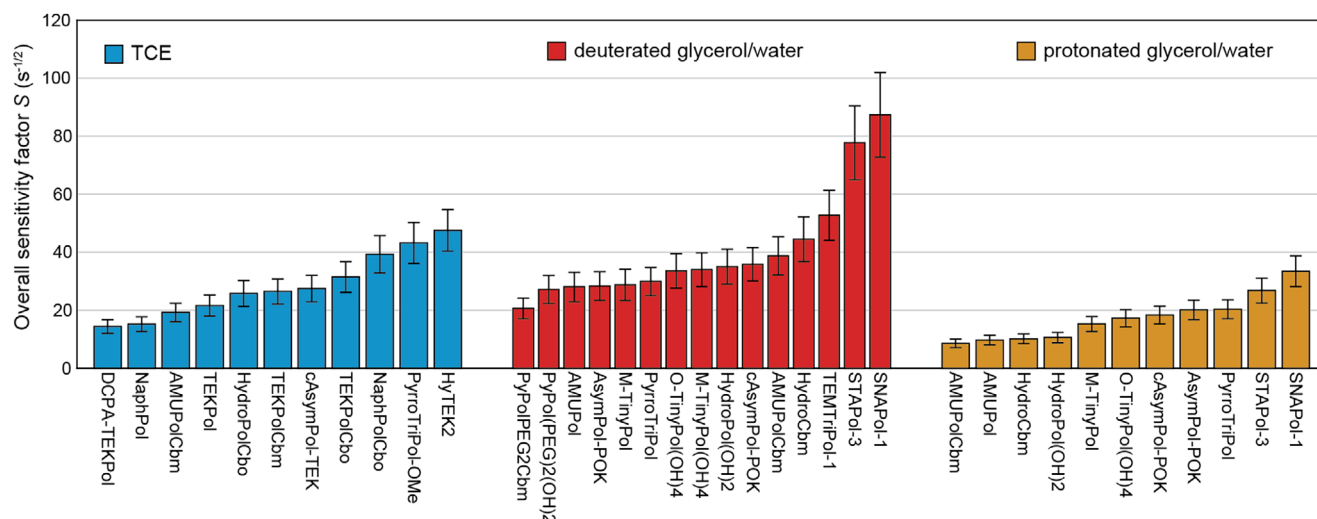


**Figure 6.** The overall sensitivity factor ( $S$ ) provided by polarizing agents in TCE (with h-BN), deuterated glycerol/water, and protonated glycerol/water, respectively, measured at 14.1 T, 100 K, and 8 kHz MAS. The values and the error analysis are detailed in the SI.

conditions, with the idea that dinitroxides are particularly suitable for intermediate field strengths. However, to the best of our knowledge, there has been no systematic comparison between hetero radicals and dinitroxides to substantiate these hypotheses. In this regard, here we measure the DNP performance of a selected group of the polarizing agents at 14.1 T. The measured values of the three key DNP parameters are shown in Figure 5, and the resultant overall sensitivity factor ( $S$ ) is shown in Figure 6. Since all the measurements at 600 MHz were performed in one experimental session, the DNP performance provided by different PAs can also be evaluated using the NMR spectral sensitivity, that is, signal-to-noise ratio per unit time. A comparison of the overall sensitivity factor  $S$  against the  $\text{SNR}/\sqrt{\text{time}}/\text{mass}$  is provided in Figure 7.

First, we see that the hetero biradicals preserve their ranking over the dinitroxides (Figure 6), albeit with a less striking difference as compared to that observed at 21.1 T. HyTEK2 and SNAPol-1 yield the highest measured values of  $S$  for TCE and glycerol/water respectively, closely followed by PyrrTriPol-OMe and STAPol-3. Meanwhile, changes in trends can be observed for the key parameters. For example, at 21.1 T, the hetero PAs show overwhelming advantages in both high contribution factors and high enhancement factors. At 21.1 T, in deuterated glycerol/water, SNAPol-1 yields an enhancement factor  $\epsilon_{\text{H}}$  almost a factor 3 higher than the best dinitroxide biradical (Figure 2b). This is however reversed at 14.1 T, where SNAPol-1 yields an enhancement factor  $\epsilon_{\text{H}}$  that is lower than the best dinitroxide biradicals (Figure 5b). However, the hetero PAs maintain higher contribution factors at 14.1 T, while that of the dinitroxide PAs are lower in general at 14.1 T than 21.1 T. (All four hetero PAs yielding  $\theta \geq 0.9$  in deuterated glycerol/water, with some measured values very close to or slightly exceeding 1.0. It is important to remember that physically, the value of the contribution factor cannot exceed 1.0, except under very specific conditions not met here.<sup>[109]</sup>) For dinitroxide PAs, from 21.1 T to 14.1 T, the increase in  $\epsilon_{\text{H}}$  is greater than the

reduction in  $\theta$ , and taken together, this yields an increase in  $S$ .

We also note here that in addition to this clear overall trend, there are some batch-to-batch variations and fluctuations in the measurements (see the SI for batch-to-batch data). As an example, there are variations in DNP key parameters observed for M-TinyPol(OH)4 and O-TinyPol(OH)4, between which the only difference is the reversed location of the nitrogen atom on the amine linker (Figure 1). Different enhancement factors and contribution factors were obtained for M-TinyPol(OH)4 ( $\epsilon_{\text{H}} = 154$ ,  $\theta = 0.37$ ) and O-TinyPol(OH)4 ( $\epsilon_{\text{H}} = 218$ ,  $\theta = 0.25$ ) in deuterated glycerol/water. This contrasts with the observation at the other two field strengths measured here, and at 18.8 T and 40 kHz MAS rate measured previously,<sup>[116]</sup> where these two dinitroxides yielded very similar DNP parameters ( $\epsilon_{\text{H}}$ ,  $T_{\text{B}}$ ,  $\theta$ ). However, more importantly, the resultant overall sensitivity factor  $S$  provided by the two PAs are identical, with  $S = 34 \text{ s}^{-1}$  for M-TinyPol(OH)4 and O-TinyPol(OH)4, which is consistent with the measurements at the other fields here, and what has been seen in the literature.<sup>[116]</sup>

In TCE and protonated glycerol/water, the gaps in the overall performance between hetero and dinitroxide PAs are also narrowed at 14.1 T as compared to those observed at 21.1 T. Again, we see that all the hetero PAs outperform the dinitroxide class in all three solvents, with the exception of PyrrTriPol in deuterated glycerol/water falling behind with a moderate  $S = 31 \text{ s}^{-1}$ . Interestingly, it returns to the top group in protonated glycerol water, just behind SNAPol-1 and STAPol-3 (Figure 6). As can be seen from their structures (Figure 1), PyrrTriPol and STAPol-3 have the same backbone, while STAPol-3 replaces the twelve methyl groups in PyrrTriPol with hydroxyl groups to improve its hydrophilicity (similar to the strategy used for SNAPol-1 on the trityl moiety). Therefore, the decreased relative performance of PyrrTriPol in deuterated glycerol/water is again most likely a result of limited aqueous solubility. The stronger solute-solvent interactions in protonated glycerol/water alleviates

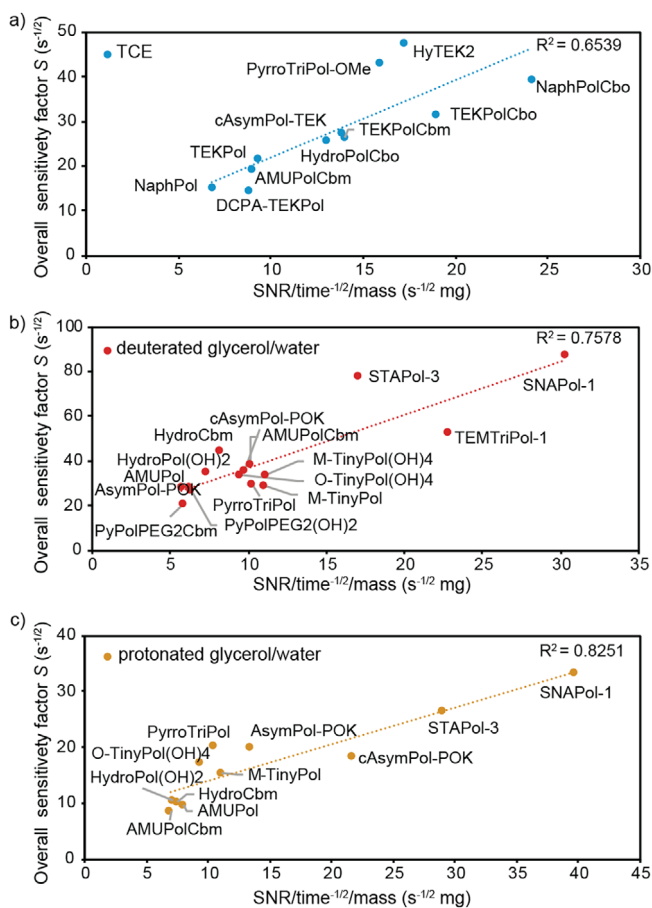


**Figure 7.** Comparison of the overall sensitivity factor ( $S$ ) against the signal-to-noise ratio per unit time per mass provided by the polarizing agents in a) TCE, b) deuterated glycerol/water, and c) protonated glycerol/water at 14.1 T, and at 100 K, 8 kHz MAS.

slightly the solubility limitation,<sup>[144]</sup> which might explain the improved relative performance of PyrroTriPol.

We note that the DNP performance of PAs in TCE at 14.1 T were measured with the addition of hexagonal boron nitride (h-BN) particles to favor reproducibility. This may impact the microwave field distribution,<sup>[8,128]</sup> whereas at 9.4 and 21.1 T, the radical solutions were measured without h-BN, but should not impact the ranking of the biradicals. Full details of sample preparation and experiments are provided in the SI.

In summary, at 14.1 T, almost the entire hetero class outperforms the dinitroxides in overall DNP performance, but by a smaller margin than at 21.1 T. Under fully protonated conditions the dinitroxides, such as AsymPol-POKs and TinyPols remain competitive with the more complex hetero biradicals.

### DNP Performance at 9.4 T

Finally, we evaluated the overall DNP performance of the PA candidates at 9.4 T, which corresponds to the most accessible and widely used field for DNP NMR today. Figure 8 shows the three key DNP parameters, and Figure 9 presents the

resultant overall sensitivity factors.

Even at 9.4 T, two hetero PAs remain amongst the PAs in the lead, again represented by HyTEK2 and SNAPol-1 for TCE and glycerol/water, respectively. Notably, hetero PAs now yield moderate enhancement factors at 9.4 T (Figure 8), approximately half of the highest enhancement factor provided by the dinitroxides (e.g.,  $\epsilon_H = 123$  for HyTEK2 vs.  $\epsilon_H = 249$  for NaphPol in TCE, and  $\epsilon_H = 165$  for SNAPol-1 vs.  $\epsilon_H = 323$  for HydroPol(OH)<sub>2</sub> in deuterated glycerol/water). However, the contribution factors of the hetero PAs vary less with the magnetic field and compensate for the lower  $\epsilon_H$  and ultimately preserve their good overall sensitivity factors. For example, in TCE, HyTEK2 yields a contribution factor  $\theta$  of 0.74 compared to dinitroxides that typically yield  $\theta$  of 0.3–0.5 (Figure 8a).

We speculate that the excellent performance of HyTEK2 across the whole range of magnetic field strengths can be ascribed to a combination of the distribution of e-e couplings and the slower electron relaxation times of the BDPA moiety<sup>[92]</sup> and the fact that the relative orientation of the  $g$ -tensors is less critical in hetero-biradicals. Indeed, unlike dinitroxides, the distance between the two  $g$ -tensors<sup>[88]</sup> remains high for any relative orientation between the BDPA and the nitroxide since, simply because the BDPA  $g$ -tensor is nearly isotropic, they always have very different  $g$ -tensor principal values.

The role of the relative orientation is visible for DCPA-TEKPol ( $S = 17 \text{ s}^{-1/2}$ ) as compared to AsymPol-TEK or cAsymPol-TEK ( $S = 34 \text{ s}^{-1/2}$ ). These biradicals possess a similar bridge and similar e-e distance, but the C = C = O conjugation in the latter two leads to a better relative orientation.<sup>[93]</sup> To obtain better biradicals for the TEKPol series, favoring the relative orientation and improving the spin diffusion appears to be key.<sup>[7]</sup> This is what is observed with the newly-developed dinitroxide PA, NaphPolCbo. It stands out as the best-performing PA in TCE at 9.4 T ( $S = 55 \text{ s}^{-1/2}$ ). NaphPolCbo is a direct development of previous studies<sup>[7,103]</sup> where sequential improvements were obtained from TEKPol ( $S = 38 \text{ s}^{-1/2}$ ) to NaphPol ( $S = 50 \text{ s}^{-1/2}$ ) which improves the <sup>1</sup>H hyperpolarization transfer pathway,<sup>[103]</sup> and from TEKPol to TEKPolCbo ( $S = 40 \text{ s}^{-1/2}$ ) that underscores the overall benefit of shorter linkers. Such linkers, similar to that of the bTurea series,<sup>[121]</sup> are known to induce stronger e-e couplings, both dipolar and exchange interactions, and in some cases better relative orientations between the  $g$ -tensors.<sup>[120]</sup> Based on this, NaphPolCbo combines these two benefits: couplings and pathways and indeed led to the best-performing PA so far at 9.4 T. This correlation between the predicted and experimental DNP performance for NaphPolCbo confirms the benefits of systematic evaluations conducted on a large collection of state-of-the-art PAs.

In deuterated glycerol/water, SNAPol-1 ( $S = 77 \text{ s}^{-1/2}$ ) also remains the best-performing radical, followed closely by M/O-TinyPol(OH)<sub>4</sub> and cAsymPol-POK ( $S \sim 70 \text{ s}^{-1/2}$ ). Similarly to HyTEK2, the preservation of the good performance of SNAPol-1 across different magnetic fields can first be attributed to their long relaxation times, the lack of dependence with respect to the  $g$ -tensor orientation and the strong e-e couplings.

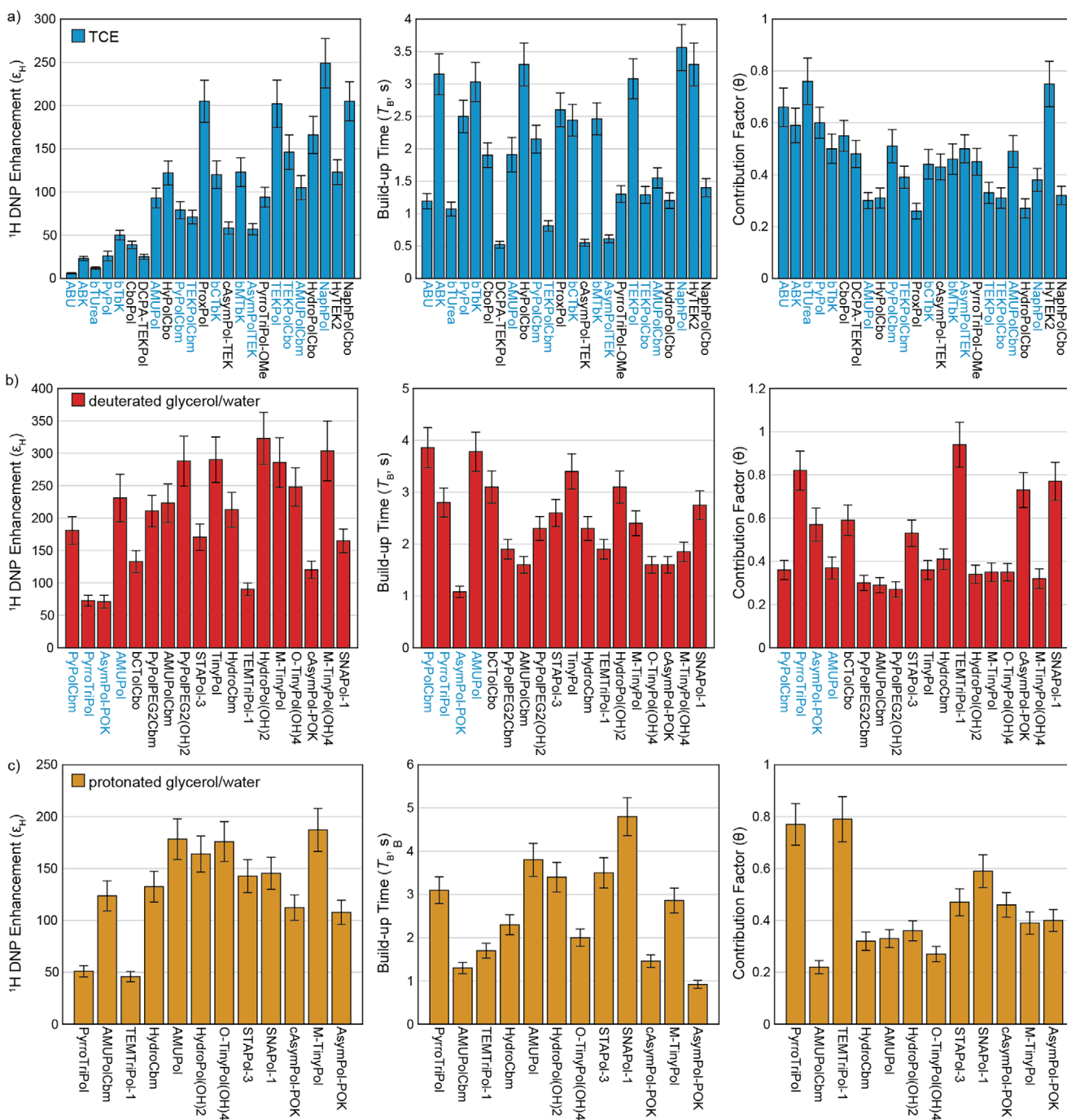


**Figure 8.** Comparison of the measured values of three key parameters,  $^1\text{H}$  DNP enhancement factor  $\epsilon_H$ , build-up time  $T_B$ , and contribution factor  $\theta$  of polarizing agents in a) TCE, b) deuterated glycerol/water, and c) protonated glycerol/water respectively, measured at 9.4 T, 100 K, and 8 kHz MAS. The values and the error analysis are detailed in the SI. The data for PAs labeled in blue are reproduced from previous work.<sup>[7]</sup>

Once cannot exclude that the relatively flexible linker, which leads to a distribution of conformations, can lead to a broad distribution of exchange couplings ( $J$ ) in a frozen glassy matrix. This was evidenced by experimental observations and numerical simulations conducted for TEMTriPol-1<sup>[92,112,126]</sup> and NATriPol,<sup>[145]</sup> which have the same linker backbone as SNAPol-1 that could explain the sustained performance at high magnetic field, but this comes with a possible drawback since overly large interactions can potentially prevent CE

rotor events.<sup>[126]</sup> This result provides insights on the potential to target the “Goldilocks” e-e interactions for a specific field strength, that is,  $^1\text{H}$  Larmor frequency, to best fulfill the CE matching condition. It also illustrates the role of the relative orientation of the  $g$ -tensors in the case of dinitroxides, and the absence of an impact in the case of hetero PAs.

Aside from the hetero PAs, from Figure 9, a large group of dinitroxides yield very similar overall sensitivity factors, despite the considerable variation in individual parameters

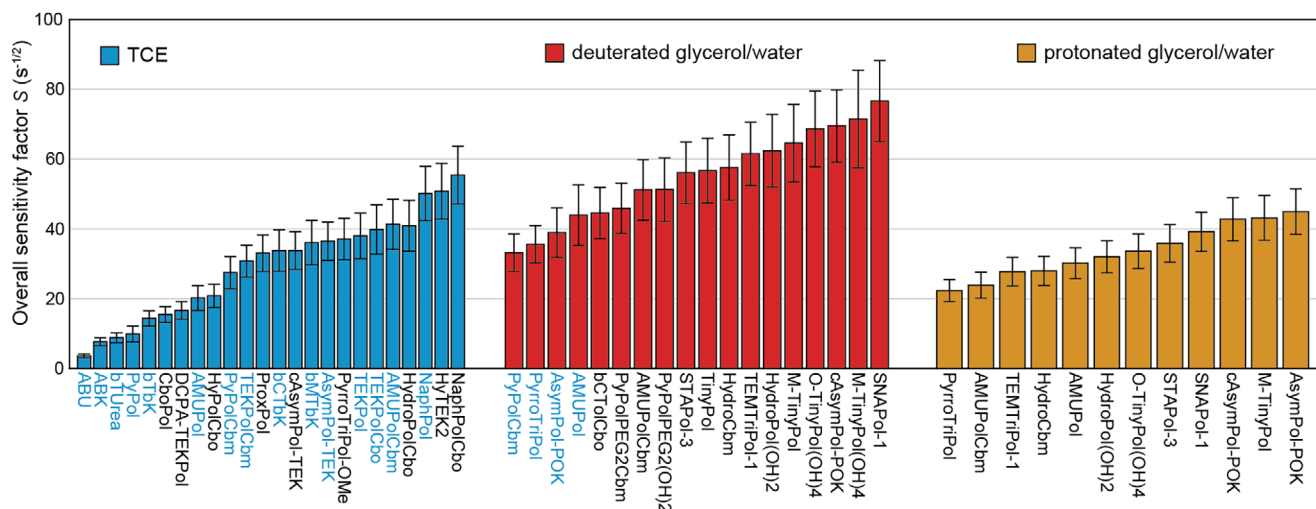


**Figure 9.** The overall sensitivity factor ( $S$ ) provided by polarizing agents in TCE, deuterated glycerol/water and protonated glycerol/water, measured at 9.4 T, 100 K, 8 kHz MAS. The values and the error analysis are detailed in the SI. The data of PAs labeled in blue are reproduced from previous work.<sup>[7]</sup>

$\varepsilon_H$ ,  $T_B$  and  $\theta$ . Again, for the benefit of the synthetic viewpoint in future PA development, we reiterate the impact of radical solubility and prevention of radical aggregation, which is reflected by the improvement in  $S$  from TinyPol (10 mM,  $S = 57 \text{ s}^{-1/2}$ ), to M/O-TinyPol(OH)4 (16 mM,  $S = 72 \text{ s}^{-1/2}$ ).

Interestingly, a significant change of the relative performance is observed in the protonated glycerol/water matrix at 9.4 T. The AsymPol-POKs and M-TinyPol now lead the DNP efficiency in proton-dense environments, slightly overtaking the DNP performance of SNAPPol-1. As mentioned previously, the high efficiency of AsymPol-POKs ( $S = 45 \text{ s}^{-1/2}$ ) in polarizing proton-rich environment is attributed to their relatively short  $T_B$  of ca. 1 s, thereby allowing an efficient turnover of polarization build-up and polarization propagation. The strong e-e coupling in AsymPol-POK has been shown to provide efficient transfer of polarization to distant protons, without being limited by the polarization transfer dynamics due to protons on the biradical.<sup>[104]</sup> This effect may contribute to the increased DNP efficiency of AsymPol-POKs in protonated glycerol/water. M-TinyPol has a  $T_B$  of 2.8 s; however, the longer  $T_B$  is mitigated by its higher signal enhancement of  $\varepsilon(\text{M-TinyPol}) = 187$  versus  $\varepsilon(\text{AsymPol}) = 108$  for a similar  $\theta$  value, altogether yielding an overall sensitivity factor  $S$  of  $43.1 \text{ s}^{-1/2}$ . The AsymPol-POKs and the M-TinyPol share a similar feature, which is their relatively short linker, leading to large electron-electron interactions; whereas a difference is the rigidity of the linker. The AsymPol-POKs utilize a conjugated double bond in the pyrroline nitroxide to increase rigidity, thereby constraining the dipolar and exchange couplings to ca. 100 and 120 MHz, respectively.<sup>[93,115]</sup> The TinyPol series on the contrary adopts a non-conjugated flexible linker, resulting in an average dipolar coupling of 47 MHz and a  $J$ -coupling distribution. For example, M-TinyPol was reported to have a distribution of  $J$  represented by  $J = 122, 28$ , and  $<5$  MHz with 44%, 44%, and 12% weightings, respectively.<sup>[97]</sup> In this case, the good performance observed from both these two series confirm the benefits of the increased e-e couplings to hyperpolarize

proton-dense environment. They also indicate that a flexible linker (i.e., a distribution of  $J$ -couplings) may not necessarily be an obstacle to obtaining good DNP performance. Indeed, a flexible linker may potentially help access larger e-e couplings, but on the other hand could also lead to less optimal matching of the relative orientations of the  $g$ -tensors.<sup>[88,117]</sup>

We further notice that the STAPol-3 in protonated glycerol/water increases its ranking compared to that in deuterated glycerol/water, closely approaching SNAPPol-1 (Figure 9). This is likely due to the larger e-e interactions reported for STAPol-3<sup>[125]</sup> than SNAPPol-1,<sup>[124]</sup> making it favorable in proton-dense systems. Another observation from Figure S5d) to S5f shows that only the AsymPol-POKs yield  $T_B$  that are consistently shorter in the protonated matrix than in the deuterated matrix. It would therefore be interesting to understand more details of the origin of this effect in order to further improve DNP efficiency in proton-dense environments, but it might be due to the fact that they polarize outside the biradical structure efficiently.<sup>[105]</sup>

### Microwave Power Dependence

A key reason for the good DNP performance of hetero PAs, in particular at higher fields, is the presence of a narrow-line moiety which enables efficient microwave saturation of the electron spin transitions, compared to that of broad-line nitroxides as previously discussed.<sup>[112,126]</sup> In dinitroxide biradicals, the wide breadth of the EPR lineshape, requires larger electron spin nutation frequencies, that is, higher power microwave sources as the field is increased. However, higher microwave powers yield higher sample temperatures which are not favorable for DNP. This problem is exacerbated with larger rotors, and it has been shown that smaller rotors can compensate for this issue.<sup>[97,116,127,146]</sup>

In contrast, the relatively long relaxation time<sup>[147]</sup> and narrow linewidth<sup>[148]</sup> of trityl and BDPA make them an excellent component to achieve more efficient saturation,

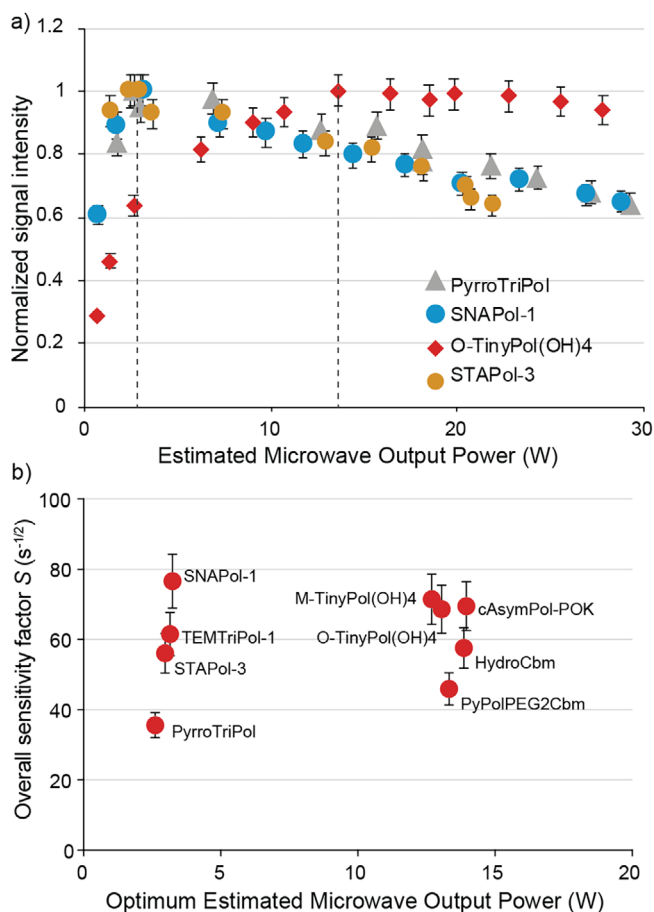


**Figure 10.** a) Microwave power dependence of the normalized signal intensities for hetero biradicals STAPol-3, PyrrroTriPol, SNAPol-1, and the dinitroxide biradical O-TinyPol(OH)4, in deuterated glycerol/water at 9.4 T, 100 K, and 8 kHz MAS. Dashed lines indicate the optimal microwave power required to yield the maximum intensity. b) Overall sensitivity factors provided by a selected collection of PAs in deuterated glycerol/water, and their respective optimal microwave powers, at 9.4 T, 100 K, and 8 kHz MAS.

even in large rotors. This advantage is reflected in the microwave power dependence, shown in Figure 10. The estimated microwave power was obtained from a measurement using a calorimeter placed halfway along the waveguide, and should be proportional to the incident power experienced by the samples. From Figure 10a, we see that the hetero PAs require only ~20% of the microwave output power to yield the optimal enhancement as compared to dinitroxide PAs, (here O-TinyPol(OH)4 was measured as a representative example). The relative microwave power necessary for optimal enhancements with hetero biradicals at 14.1 and 21.1 T increases to around 60% and 100%, respectively, as compared to dinitroxides. The gradual reduction in signal intensity seen in Figure 10a at higher microwave power is ascribed to the sample temperature rising. (This effect has been recently simulated.)<sup>[126]</sup> Here, maximum cooling power was used throughout and no temperature compensation was conducted between the microwave on and off experiments. The measured sample temperature as a function of microwave output

power is shown in Figure S1. We note the slight differences in the optimal microwave power for the same class of PAs shown in Figure 10b are likely due to the different linewidth and/or saturation factors of the radicals. For example, PyrrroTriPol shows an optimal power slightly lower than TEMTriPol-1 and SNAPol-1, possibly because the trityl linewidth is less broadened in PyrrroTriPol compared to the other two, thereby improving the efficiency slightly, as previously reported.<sup>[126]</sup> The power dependence is in agreement with previous work on TEMTriPol-I at 9.4 T<sup>[112]</sup> or the PyrrroTriPols at 14.1 T in TCE and glycerol/water.<sup>[126]</sup> This systematic analysis further confirms that the significantly reduced microwave power required for hetero PAs at 9.4 T will be an advantage on DNP NMR systems with low power sources, for example, using klystrons,<sup>[126,149,150]</sup> or solid-state sources.<sup>[151]</sup>

## Conclusion

In summary, a collection of 32 biradicals for CE DNP was compared, including 26 dinitroxides and 6 hetero biradicals, selected based upon the best-performing candidates currently at play,<sup>[7,90,92–94,97,102,103,115,116,124–126,133]</sup> and newly developed PAs that capitalize on the design principles established from previous studies.<sup>[7,91,121]</sup> This work marks the first example where the two classes of hetero and dinitroxide biradicals are directly compared across variable magnetic field strengths, and in different proton concentrations. Detailed key DNP parameters, namely the <sup>1</sup>H DNP enhancement factor ( $\epsilon_H$ ), the build-up time of the polarization ( $TB$ ), and the contribution factor ( $\theta$ ) are reported, providing quantification of the overall DNP performance.

First, we find that all the hetero PAs outperform the dinitroxide class at 21.1 T (Figure 3), the highest MAS DNP NMR field available today. Then, SNAPol-1 and HyTEK2, the best candidates among the hetero class for aqueous and organic solvents respectively at 21.1 T, remain among the best PAs at both 14.1 T (Figure 6) and at 9.4 T (Figure 9) in media with modest protonation levels. Their moderate enhancement factors at 9.4 T are mitigated by the high contribution factors (i.e., limited depolarization effect), thereby retaining their competence as compared to the dinitroxide PAs at this field. This robust performance of SNAPol-1 and HyTEK-2 across different field strengths is attributed to the long relaxation times of the trityl or BDPA, to their strong e-e interactions and the fact they are nearly insensitive to the relative orientation of the  $g$ -tensors. It is also possible that their flexible linker allows access to a distribution of e-e couplings making their performance robust across magnetic fields. This in turn indicates the potential to tailor the e-e coupling strengths for a given target field to maximize the DNP efficiency in the future. Furthermore, the study confirms another advantageous feature of hetero PAs, which is their substantially lower requirement for microwave power (Figure 10).<sup>[112,126]</sup> This feature could be of particular interest to studies where only low power sources are available.<sup>[126]</sup>

At 9.4 T, it is worth noting some dinitroxide candidates that stand out. Specifically, NaphPolCbo, a new biradical designed by combining results from previous studies,<sup>[7,103]</sup>

provides the highest DNP efficiency in organic solvents. AsymPol-POKs and M-TinyPol are the best-performing dinitroxide PAs in the proton-dense glycerol/water matrix at 9.4 T. The persistent lower polarization build-up time of AsymPol-POKs in the protonated matrix as compared to the deuterated matrix, in stark contrast to the other PAs, remains an interesting topic to explore as it explains their relatively very good performance in proton-dense media at all fields for the dinitroxide class.

Given the increasing range applications of DNP NMR that has gone hand in hand with the development of the instrumentation, there is still undeniable value in optimizing polarizing agents that are ideally tailored for variable magnetic fields. With many design principles identified today, further optimization of PAs is a complex process that requires fine tuning of multiple-factors. It is challenging to predict a radical that exhibits, for example, high  $\epsilon_H$ , low  $TB$ , and high  $\theta$  simultaneously. Our attempt at systematic evaluation carried out here therefore provides key useful insights on approaching such ideal PAs.

Overall, with the extensive studies in the pursuit of optimal PA thus far leading to a large number of polarizing agents, our work clearly highlights the outstanding performance and potential of hetero PAs, not only in the high field regimes that hetero PAs were designed for but also at intermediate field strengths. To date, the current collection of hetero PAs is far outnumbered by dinitroxides, primarily due to their efficiency at 9.4 T for which spectrometers are more common than at higher field. With the results here, and the need to expand DNP to microwave sources with lower power, we anticipate considerable efforts will now be diverted towards the development of new efficient, stable and soluble hetero PAs at 9.4 T.

As NMR instrumentation today reaches beyond 1.2 GHz, bridging the gap between CE DNP efficiency and ultra-high magnetic fields will no doubt maximize the impact of DNP NMR for the broader community, and further optimization of high-field polarizing agents is essential to achieving this goal.

## Acknowledgements

This work was supported by Swiss National Science Foundation Grant No. 200020\_212046, EU H2020-INFRAIA Grant No. 101008500, and French National Research Agency grant No ANR-22-CE09-0017-01, France 2023 A\*MIDEX AMX-22-RE-AB-023. The National High Magnetic Field Laboratory (NHMFL) is supported by the National Science Foundation through NSF/DMR-2128556 and the State of Florida. A portion of this work was supported by National Institutes of Health Grant RM1-GM148766, the National Natural Science Foundation of China (Nos. 22174099 and 21871210), and the Icelandic Research Fund, grant No. 239662 (SthS).

Open access publishing facilitated by Ecole polytechnique federale de Lausanne, as part of the Wiley - Ecole polytechnique federale de Lausanne agreement via the Consortium Of Swiss Academic Libraries.

## Conflict of Interests

The authors declare no conflict of interest.

## Data Availability Statement

The data that support the findings of this study are openly available in Zenodo at <https://doi.org/10.1111/1522-2675.123456>, reference number 123456.

**Keywords:** Biradicals • Dynamic nuclear polarization • Magic angle spinning • Polarization agents • Solid-state nuclear magnetic resonance

- [1] B. Reif, S. E. Ashbrook, L. Emsley, M. Hong, *Nat. Rev. Methods Primers* **2021**, *1*, 2.
- [2] J.-H. Ardenkjaer-Larsen, G. S. Boebinger, A. Comment, S. Duckett, A. S. Edison, F. Engelke, C. Griesinger, R. G. Griffin, C. Hilty, H. Maeda, G. Parigi, T. Prisner, E. Ravera, J. Van Bentum, S. Vega, A. Webb, C. Luchinat, H. Schwalbe, L. Frydman, *Angew. Chem. Int. Ed.* **2015**, *54*, 9162–9185.
- [3] A. S. Lilly Thankamony, J. J. Wittmann, M. Kaushik, B. Corzilius, *Prog. Nucl. Magn. Reson. Spectrosc.* **2017**, *102-103*, 120–195.
- [4] J. Eills, D. Budker, S. Cavagnero, E. Y. Chekmenev, S. J. Elliott, S. Jannin, A. Lesage, J. Matysik, T. Meersmann, T. Prisner, J. A. Reimer, H. Yang, I. V. Koptuyug, *Chem. Rev.* **2023**, *123*, 1417–1551.
- [5] G. Menzildjian, J. Schlagnitweit, G. Casano, O. Ouari, D. Gajan, A. Lesage, *Chem. Sci.* **2023**, *14*, 6120–6148.
- [6] B. Corzilius, *Annu. Rev. Phys. Chem.* **2020**, *71*, 143–170.
- [7] A. Venkatesh, G. Casano, R. Wei, Y. Rao, H. Lingua, H. Karoui, M. Yulikov, O. Ouari, L. Emsley, *Angew. Chem. Int. Ed.* **2024**, *63*, e202317337.
- [8] M. P. Hanrahan, Y. Chen, R. Blome-Fernández, J. L. Stein, G. F. Pach, M. A. S. Adamson, N. R. Neale, B. M. Cossairt, J. Vela, A. J. Rossini, *J. Am. Chem. Soc.* **2019**, *141*, 15532–15546.
- [9] Y. Chen, R. W. Dorn, M. P. Hanrahan, L. Wei, R. Blome-Fernández, A. M. Medina-Gonzalez, M. A. S. Adamson, A. H. Flintgruber, J. Vela, A. J. Rossini, *J. Am. Chem. Soc.* **2021**, *143*, 8747–8760.
- [10] O. Segura Lecina, M. A. Hope, A. Venkatesh, S. Björgvinsdóttir, K. Rossi, A. Loiudice, L. Emsley, R. Buonsanti, *J. Am. Chem. Soc.* **2022**, *144*, 3998–4008.
- [11] D. Lee, M. Wolska-Pietkiewicz, S. Badoni, A. Grala, J. Lewiński, G. De Paëpe, *Angew. Chem. Int. Ed.* **2019**, *58*, 17163–17168.
- [12] S. Badoni, M. Terlecki, S. Carret, J.-F. Poisson, T. Charpentier, H. Okuno, M. Wolska-Pietkiewicz, D. Lee, J. Lewiński, G. De Paëpe, *J. Am. Chem. Soc.* **2024**, *146*, 27655–27667.
- [13] N. Olejnik-Fehér, M. Jędrzejewska, M. Wolska-Pietkiewicz, D. Lee, G. De Paëpe, J. Lewiński, *Small* **2024**, *20*, 2309984.
- [14] M. Terlecki, S. Badoni, M. K. Leszczyński, S. Gierlotka, I. Justyniak, H. Okuno, M. Wolska-Pietkiewicz, D. Lee, G. De Paëpe, J. Lewiński, *Adv. Funct. Mater.* **2021**, *31*, 2105318.
- [15] D. Lee, H. Takahashi, A. S. L. Thankamony, J.-P. Dacquin, M. Bardet, O. Lafon, G. De Paëpe, *J. Am. Chem. Soc.* **2012**, *134*, 18491–18494.
- [16] P. Wolf, M. Valla, A. J. Rossini, A. Comas-Vives, F. Núñez-Zarur, B. Malaman, A. Lesage, L. Emsley, C. Copéret, I. Hermans, *Angew. Chem. Int. Ed.* **2014**, *53*, 10179–10183.
- [17] A. S. Lilly Thankamony, C. Lion, F. Pourpoint, B. Singh, A. J. Perez Linde, D. Carnevale, G. Bodenhausen, H. Vezin,

- O. Lafon, V. Polshettiwar, *Angew. Chem. Int. Ed.* **2015**, *54*, 2190–2193.
- [18] T. Kobayashi, F. A. Perras, I. I. Slowing, A. D. Sadow, M. Pruski, *ACS Catal.* **2015**, *5*, 7055–7062.
- [19] J. C. Mohandas, E. Abou-Hamad, E. Callens, M. K. Samantaray, D. Gajan, A. Gurinov, T. Ma, S. Ould-Chikh, A. S. Hoffman, B. C. Gates, J.-M. Basset, *Chem. Sci.* **2017**, *8*, 5650–5661.
- [20] T. Kobayashi, M. Pruski, *ACS Catal.* **2019**, *9*, 7238–7249.
- [21] A. Venkatesh, A. Lund, L. Rochlitz, R. Jabbour, C. P. Gordon, G. Menzildjian, J. Viger-Gravel, P. Berruyer, D. Gajan, C. Copéret, A. Lesage, A. J. Rossini, *J. Am. Chem. Soc.* **2020**, *142*, 18936–18945.
- [22] Z. Wang, L. A. Völker, T. C. Robinson, N. Kaefter, G. Menzildjian, R. Jabbour, A. Venkatesh, D. Gajan, A. J. Rossini, C. Copéret, A. Lesage, *J. Am. Chem. Soc.* **2022**, *144*, 21530–21543.
- [23] T. Wolf, S. Kumar, H. Singh, T. Chakrabarty, F. Aussenac, A. I. Frenkel, D. T. Major, M. Leskes, *J. Am. Chem. Soc.* **2019**, *141*, 451–462.
- [24] M. A. Hope, B. L. D. Rinkel, A. B. Gunnarsdóttir, K. Märker, S. Menkin, S. Paul, I. V. Sergeev, C. P. Grey, *Nat. Commun.* **2020**, *11*, 2224.
- [25] S. Haber, M. Leskes, *Solid State Nucl. Magn. Reson.* **2022**, *117*, 101763.
- [26] A. Maity, A. Svirinovsky-Arbeli, Y. Buganim, C. Oppenheim, M. Leskes, *Nat. Commun.* **2024**, *15*, 9956.
- [27] A. Mishra, M. A. Hope, M. Almalki, L. Pfeifer, S. M. Zakeeruddin, M. Grätzel, L. Emsley, *J. Am. Chem. Soc.* **2022**, *144*, 15175–15184.
- [28] R. P. Sangodkar, B. J. Smith, D. Gajan, A. J. Rossini, L. R. Roberts, G. P. Funkhouser, A. Lesage, L. Emsley, B. F. Chmelka, *J. Am. Chem. Soc.* **2015**, *137*, 8096–8112.
- [29] A. Kumar, B. J. Walder, A. Kunhi Mohamed, A. Hofstetter, B. Srinivasan, A. J. Rossini, K. Scrivener, L. Emsley, P. Bowen, *J. Phys. Chem. C* **2017**, *121*, 17188–17196.
- [30] A. Kunhi Mohamed, P. Moutzouri, P. Berruyer, B. J. Walder, J. Siramanont, M. Harris, M. Negroni, S. C. Galmarini, S. C. Parker, K. L. Scrivener, L. Emsley, P. Bowen, *J. Am. Chem. Soc.* **2020**, *142*, 11060–11071.
- [31] A. Morales-Melgares, Z. Casar, P. Moutzouri, A. Venkatesh, M. Cordova, A. Kunhi Mohamed, K. L. Scrivener, P. Bowen, L. Emsley, *J. Am. Chem. Soc.* **2022**, *144*, 22915–22924.
- [32] B. J. Walder, C. Berk, W.-C. Liao, A. J. Rossini, M. Schwarzwälder, U. Pradere, J. Hall, A. Lesage, C. Copéret, L. Emsley, *ACS Cent. Sci.* **2019**, *5*, 515–523.
- [33] H. Takahashi, S. Hediger, G. De Paëpe, *Chem. Commun.* **2013**, *49*, 9479.
- [34] M. Kaushik, T. Bahrenberg, T. V. Can, M. A. Caporini, R. Silvers, J. Heiliger, A. A. Smith, H. Schwalbe, R. G. Griffin, B. Corzilius, *Phys. Chem. Chem. Phys.* **2016**, *18*, 27205–27218.
- [35] S. Lange, W. T. Franks, N. Rajagopalan, K. Döring, M. A. Geiger, A. Linden, B.-J. van Rossum, G. Kramer, B. Bukau, H. Oschkinat, *Sci. Adv.* **2016**, *2*, e1600379.
- [36] A. N. Smith, K. Märker, T. Piretra, J. C. Boatz, I. Matlahov, R. Kodali, S. Hediger, P. C. A. van der Wel, G. De Paëpe, *J. Am. Chem. Soc.* **2018**, *140*, 14576–14580.
- [37] K. Jaudzems, T. Polenova, G. Pintacuda, H. Oschkinat, A. Lesage, *J. Struct. Biol.* **2019**, *206*, 90–98.
- [38] S. Bahri, R. Silvers, B. Michael, K. Jaudzems, D. Lalli, G. Casano, O. Ouari, A. Lesage, G. Pintacuda, S. Linse, R. G. Griffin, *Proc. Natl. Acad. Sci.* **2022**, *119*, e2114413119.
- [39] A. Lends, N. Birlirakis, X. Cai, A. Daskalov, J. Shenoy, M. B. Abdul-Shukoor, M. Berbon, F. Ferrage, Y. Liu, A. Loquet, K. O. Tan, *J. Biomol. NMR* **2023**, *77*, 121–130.
- [40] X. Kang, A. Kirui, M. C. Dickwella Widanage, F. Mentink-Vigier, D. J. Cosgrove, T. Wang, *Nat. Commun.* **2019**, *10*, 347.
- [41] P. Berruyer, M. Gericke, P. Moutzouri, D. Jakobi, M. Bardet, L. Karlson, S. Schantz, T. Heinze, L. Emsley, *Carbohydr. Polym.* **2021**, *262*, 117944.
- [42] A. Kirui, W. Zhao, F. Deligey, H. Yang, X. Kang, F. Mentink-Vigier, T. Wang, *Nat. Commun.* **2022**, *13*, 538.
- [43] L. D. Fernando, W. Zhao, I. Gautam, A. Ankur, T. Wang, *Structure* **2023**, *31*, 1375–1385.
- [44] A. Poulhazan, A. A. Arnold, F. Mentink-Vigier, A. Muszyński, P. Azadi, A. Halim, S. Y. Vakhrushev, H. J. Joshi, T. Wang, D. E. Warschawski, I. Marcotte, *Nat. Commun.* **2024**, *15*, 986.
- [45] H. Takahashi, D. Lee, L. Dubois, M. Bardet, S. Hediger, G. De Paëpe, *Angew. Chem. Int. Ed.* **2012**, *51*, 11766–11769.
- [46] A. Kumar, H. Durand, E. Zeno, C. Balsollier, B. Watbled, C. Sillard, S. Fort, I. Baussanne, N. Belgacem, D. Lee, S. Hediger, M. Demeunynck, J. Bras, G. De Paëpe, *Chem. Sci.* **2020**, *11*, 3868–3877.
- [47] A. Kumar, B. Watbled, I. Baussanne, S. Hediger, M. Demeunynck, G. De Paëpe, *Commun. Chem.* **2023**, *6*, 58.
- [48] M. Kaplan, A. Cukkemane, G. C. P. Van Zundert, S. Narasimhan, M. Daniëls, D. Mance, G. Waksman, A. M. J. J. Bonvin, R. Fronzes, G. E. Folkers, M. Baldus, *Nat. Methods* **2015**, *12*, 649–652.
- [49] K. K. Frederick, V. K. Michaelis, B. Corzilius, T.-C. Ong, A. C. Jacavone, R. G. Griffin, S. Lindquist, *Cell* **2015**, *163*, 620–628.
- [50] J. Medeiros-Silva, S. Jehkmane, A. L. Paioni, K. Gawarecka, M. Baldus, E. Swiezewska, E. Breukink, M. Weingarh, *Nat. Commun.* **2018**, *9*, 3963.
- [51] B. J. Albert, C. K. Gao, E. L. Sesti, E. P. Saliba, N. Alaniva, F. J. Scott, S. T. Sigurdsson, A. B. Barnes, *Biochem* **2018**, *57*, 4741–4746.
- [52] J. Schlagnitweit, S. Friebe Sandoz, A. Jaworski, I. Guzzetti, F. Aussenac, R. J. Carbajo, E. Chiarparin, A. J. Pell, K. Petzold, *ChemBioChem* **2019**, *20*, 2474–2478.
- [53] P. T. Judge, E. L. Sesti, L. E. Price, B. J. Albert, N. Alaniva, E. P. Saliba, T. Halbritter, S. T. Sigurdsson, G. B. Kyei, A. B. Barnes, *J. Phys. Chem. B* **2020**, *124*, 2323–2330.
- [54] R. Ghosh, Y. Xiao, J. Kragelj, K. K. Frederick, *J. Am. Chem. Soc.* **2021**, *143*, 18454–18466.
- [55] S. A. Overall, A. B. Barnes, *Front. Mol. Biosci.* **2021**, *8*, 743829.
- [56] B. E. Ackermann, B. J. Lim, N. Elathram, S. Narayanan, G. T. Debelouchina, *ChemBioChem* **2022**, *23*, e202200577.
- [57] Y. Rao, P. Berruyer, A. Bertarello, A. Venkatesh, M. Mazzanti, L. Emsley, *J. Phys. Chem. Lett.* **2024**, *15*, 11601–11607.
- [58] A. Bertarello, P. Berruyer, M. Artelsmair, C. S. Elmore, S. Heydarkhan-Hagvall, M. Schade, E. Chiarparin, S. Schantz, L. Emsley, *J. Am. Chem. Soc.* **2022**, *144*, 6734–6741.
- [59] D. Lee, G. Monin, N. T. Duong, I. Z. Lopez, M. Bardet, V. Mareau, L. Gonon, G. De Paëpe, *J. Am. Chem. Soc.* **2014**, *136*, 13781–13788.
- [60] A. J. Rossini, C. M. Widdifield, A. Zagdoun, M. Lelli, M. Schwarzwälder, C. Copéret, A. Lesage, L. Emsley, *J. Am. Chem. Soc.* **2014**, *136*, 2324–2334.
- [61] Q. Z. Ni, F. Yang, T. V. Can, I. V. Sergeev, S. M. D'Addio, S. K. Jawla, Y. Li, M. P. Lipert, W. Xu, R. T. Williamson, A. Leone, R. G. Griffin, Y. Su, *J. Phys. Chem. B* **2017**, *121*, 8132–8141.
- [62] J. Viger-Gravel, A. Schantz, A. C. Pinon, A. J. Rossini, S. Schantz, L. Emsley, *J. Phys. Chem. B* **2018**, *122*, 2073–2081.
- [63] M. Cordova, M. Balodis, A. Hofstetter, F. Paruzzo, S. O. Nilsson Lill, E. S. E. Eriksson, P. Berruyer, B. Simões de Almeida, M. J. Quayle, S. T. Norberg, A. Svensk Ankarberg, S. Schantz, L. Emsley, *Nat. Commun.* **2021**, *12*, 2964.

- [64] M. Juramy, R. Chèvre, P. Cerreia Vioglio, F. Ziarelli, E. Besson, S. Gastaldi, S. Viel, P. Thureau, K. D. M. Harris, G. Mollica, *J. Am. Chem. Soc.* **2021**, *143*, 6095–6103.
- [65] P. Berruyer, P. Moutzouri, M. Gericke, D. Jakobi, M. Bardet, T. Heinze, L. Karlson, S. Schantz, L. Emsley, *Macromolecules* **2022**, *55*, 2952–2958.
- [66] Y. Chen, J. Mi, A. J. Rossini, *Chem. Sci.* **2023**, *14*, 11296–11299.
- [67] M. Cordova, P. Moutzouri, S. O. Nilsson Lill, A. Cousen, M. Kearns, S. T. Norberg, A. Svensk Ankarberg, J. McCabe, A. C. Pinon, S. Schantz, L. Emsley, *Nat. Commun.* **2023**, *14*, 5138.
- [68] P. Berruyer, M. Lindkvist, S. Gracin, T. Starciuc, A. Bertarello, B. Busi, S. Schantz, L. Emsley, *Mol. Pharmaceutics* **2023**, *20*, 5682–5689.
- [69] A. B. Barnes, G. De Paëpe, P. C. A. van der Wel, K. N. Hu, C. G. Joo, V. S. Bajaj, M. L. Mak-Jurkauskas, J. R. Sirigiri, J. Herzfeld, R. J. Temkin, R. G. Griffin, *Appl. Magn. Reson.* **2008**, *34*, 237–263.
- [70] T. Maly, G. T. Debelouchina, V. S. Bajaj, K.-N. Hu, C.-G. Joo, M. L. Mak-Jurkauskas, J. R. Sirigiri, P. C. A. Van Der Wel, J. Herzfeld, R. J. Temkin, R. G. Griffin, *J. Chem. Phys.* **2008**, *128*, 052211.
- [71] M. Rosay, L. Tometich, S. Pawsey, R. Bader, R. Schauwecker, M. Blank, P. M. Borchard, S. R. Cauffman, K. L. Felch, R. T. Weber, R. J. Temkin, R. G. Griffin, W. E. Maas, *Phys. Chem. Chem. Phys.* **2010**, *12*, 5850.
- [72] A. J. Rossini, A. Zagdoun, M. Lelli, A. Lesage, C. Copéret, L. Emsley, *Acc. Chem. Res.* **2013**, *46*, 1942–1951.
- [73] Q. Z. Ni, E. Daviso, T. V. Can, E. Markhasin, S. K. Jawla, T. M. Swager, R. J. Temkin, J. Herzfeld, R. G. Griffin, *Acc. Chem. Res.* **2013**, *46*, 1933–1941.
- [74] P. C. A. van der Wel, K. N. Hu, J. Lewandowski, R. G. Griffin, *J. Am. Chem. Soc.* **2006**, *128*, 10840–10846.
- [75] A. C. Pinon, J. Schlagnitweit, P. Berruyer, A. J. Rossini, M. Lelli, E. Socie, M. Tang, T. Pham, A. Lesage, S. Schantz, L. Emsley, *J. Phys. Chem. C* **2017**, *121*, 15993–16005.
- [76] F. Mentink-Vigier, S. Vega, G. De Paëpe, *Phys. Chem. Chem. Phys.* **2017**, *19*, 3506–3522.
- [77] F. A. Perras, M. Pruski, *J. Chem. Phys.* **2018**, *149*, 154202.
- [78] F. A. Perras, M. Raju, S. L. Carnahan, D. Akbarian, A. C. T. van Duin, A. J. Rossini, M. Pruski, *J. Phys. Chem. Lett.* **2020**, *11*, 5655–5660.
- [79] N. A. Prisco, A. C. Pinon, L. Emsley, B. F. Chmelka, *Phys. Chem. Chem. Phys.* **2021**, *23*, 1006–1020.
- [80] E. Bouleau, P. Saint-Bonnet, F. Mentink-Vigier, H. Takahashi, J. F. Jacquot, M. Bardet, F. Aussenac, A. Pureau, F. Engelke, S. Hediger, D. Lee, G. De Paëpe, *Chem. Sci.* **2015**, *6*, 6806–6812.
- [81] D. Lee, E. Bouleau, P. Saint-Bonnet, S. Hediger, G. De Paëpe, *J. Magn. Reson.* **2016**, *264*, 116–124.
- [82] Y. Matsuki, T. Sugishita, T. Fujiwara, *J. Phys. Chem. C* **2020**, *124*, 18609–18614.
- [83] S. Paul, E. Bouleau, Q. Reynard-Feytis, J.-P. Arnaud, F. Bancel, B. Rollet, P. Dalban-Moreynas, C. Reiter, A. Pureau, F. Engelke, S. Hediger, G. De Paëpe, *J. Magn. Reson.* **2023**, *356*, 107561.
- [84] K.-N. Hu, H.-h. Yu, T. M. Swager, R. G. Griffin, *J. Am. Chem. Soc.* **2004**, *126*, 10844–10845.
- [85] G. Casano, H. Karoui, O. Ouari, *eMagRes* **2018**, *7*, 195–208.
- [86] Y. Matsuki, T. Maly, O. Ouari, H. Karoui, F. Le Moigne, E. Rizzato, S. Lyubenova, J. Herzfeld, T. Prisner, P. Tordo, R. G. Griffin, *Angew. Chem. Int. Ed.* **2009**, *48*, 4996–5000.
- [87] M. K. Kiesewetter, B. Corzilius, A. A. Smith, R. G. Griffin, T. M. Swager, *J. Am. Chem. Soc.* **2012**, *134*, 4537–4540.
- [88] F. Mentink-Vigier, *Phys. Chem. Chem. Phys.* **2020**, *22*, 3643–3652.
- [89] A. Zagdoun, G. Casano, O. Ouari, G. Lapadula, A. J. Rossini, M. Lelli, M. Baffert, D. Gajan, L. Veyre, W. E. Maas, M. Rosay, R. T. Weber, C. Thieuleux, C. Coperet, A. Lesage, P. Tordo, L. Emsley, *J. Am. Chem. Soc.* **2012**, *134*, 2284–2291.
- [90] A. Zagdoun, G. Casano, O. Ouari, M. Schwarzwälder, A. J. Rossini, F. Aussenac, M. Yulikov, G. Jeschke, C. Copéret, A. Lesage, P. Tordo, L. Emsley, *J. Am. Chem. Soc.* **2013**, *135*, 12790–12797.
- [91] D. J. Kubicki, G. Casano, M. Schwarzwälder, S. Abel, C. Sauvée, K. Ganesan, M. Yulikov, A. J. Rossini, G. Jeschke, C. Copéret, A. Lesage, P. Tordo, O. Ouari, L. Emsley, *Chem. Sci.* **2016**, *7*, 550–558.
- [92] G. Mathies, M. A. Caporini, V. K. Michaelis, Y. Liu, K.-N. Hu, D. Mance, J. L. Zweier, M. Rosay, M. Baldus, R. G. Griffin, *Angew. Chem. Int. Ed.* **2015**, *54*, 11770–11774.
- [93] F. Mentink-Vigier, I. Marin-Montesinos, A. P. Jagtap, T. Halbritter, J. van Tol, S. Hediger, D. Lee, S. T. Sigurdsson, G. De Paëpe, *J. Am. Chem. Soc.* **2018**, *140*, 11013–11019.
- [94] D. Wisser, G. Karthikeyan, A. Lund, G. Casano, H. Karoui, M. Yulikov, G. Menzildjian, A. C. Pinon, A. Pureau, F. Engelke, S. R. Chaudhari, D. Kubicki, A. J. Rossini, I. B. Moroz, D. Gajan, C. Copéret, G. Jeschke, M. Lelli, L. Emsley, A. Lesage, O. Ouari, *J. Am. Chem. Soc.* **2018**, *140*, 13340–13349.
- [95] W. Zhai, Y. Feng, H. Liu, A. Rockenbauer, D. Mance, S. Li, Y. Song, M. Baldus, Y. Liu, *Chem. Sci.* **2018**, *9*, 4381–4391.
- [96] A. Equbal, K. Tagami, S. Han, *Phys. Chem. Chem. Phys.* **2020**, *22*, 13569–13579.
- [97] A. Lund, G. Casano, G. Menzildjian, M. Kaushik, G. Stevanato, M. Yulikov, R. Jabbour, D. Wisser, M. Renom-Carrasco, C. Thieuleux, F. Bernada, H. Karoui, D. Siri, M. Rosay, I. V. Sergeev, D. Gajan, M. Lelli, L. Emsley, O. Ouari, A. Lesage, *Chem. Sci.* **2020**, *11*, 2810–2818.
- [98] K. R. Thurber, R. Tycko, *J. Chem. Phys.* **2012**, *137*, 084508.
- [99] F. Mentink-Vigier, Ü. Akbey, H. Oschkinat, S. Vega, A. Feintuch, *J. Magn. Reson.* **2015**, *258*, 102–120.
- [100] C. Song, K.-N. Hu, C.-G. Joo, T. M. Swager, R. G. Griffin, *J. Am. Chem. Soc.* **2006**, *128*, 11385–11390.
- [101] G. Stevanato, G. Casano, D. J. Kubicki, Y. Rao, L. Esteban Hofer, G. Menzildjian, H. Karoui, D. Siri, M. Cordova, M. Yulikov, G. Jeschke, M. Lelli, A. Lesage, O. Ouari, L. Emsley, *J. Am. Chem. Soc.* **2020**, *142*, 16587–16599.
- [102] R. Harrabi, T. Halbritter, S. Alarab, S. Chatterjee, M. Wolska-Pietkiewicz, K. K. Damodaran, J. Van Tol, D. Lee, S. Paul, S. Hediger, S. T. Sigurdsson, F. Mentink-Vigier, G. De Paëpe, *Phys. Chem. Chem. Phys.* **2024**, *26*, 5669–5682.
- [103] A. Venkatesh, G. Casano, Y. Rao, F. De Biasi, F. A. Perras, D. J. Kubicki, D. Siri, S. Abel, H. Karoui, M. Yulikov, O. Ouari, L. Emsley, *Angew. Chem. Int. Ed.* **2023**, *62*, e202304844.
- [104] S. Chatterjee, A. Venkatesh, S. T. Sigurdsson, F. Mentink-Vigier, *J. Phys. Chem. Lett.* **2024**, *15*, 2160–2168.
- [105] S. Chatterjee, F. J. Scott, S. T. Sigurdsson, A. Venkatesh, F. Mentink-Vigier, *J. Phys. Chem. Lett.* **2025**, *16*, 635–641.
- [106] A. Zagdoun, A. J. Rossini, D. Gajan, A. Bourdolle, O. Ouari, M. Rosay, W. E. Maas, P. Tordo, M. Lelli, L. Emsley, A. Lesage, C. Copéret, *Chem. Commun.* **2012**, *48*, 654–656.
- [107] A. J. Rossini, A. Zagdoun, M. Lelli, D. Gajan, F. Rascón, M. Rosay, W. E. Maas, C. Copéret, A. Lesage, L. Emsley, *Chem. Sci.* **2012**, *3*, 108–115.
- [108] O. Lafon, A. S. L. Thankamony, T. Kobayashi, D. Carnevale, V. Vitzthum, I. I. Slowing, K. Kandel, H. Vezin, J. P. Amoureux, G. Bodenhausen, M. Pruski, *J. Phys. Chem. C* **2013**, *117*, 1375–1382.
- [109] K. R. Thurber, R. Tycko, *J. Chem. Phys.* **2014**, *140*, 184201.
- [110] B. Corzilius, L. B. Andreas, A. A. Smith, Q. Z. Ni, R. G. Griffin, *J. Magn. Reson.* **2014**, *240*, 113–123.
- [111] F. Mentink-Vigier, S. Paul, D. Lee, A. Feintuch, S. Hediger, S. Vega, G. De Paëpe, *Phys. Chem. Chem. Phys.* **2015**, *17*, 21824–21836.

- [112] F. Mentink-Vigier, G. Mathies, Y. Liu, A.-L. Barra, M. A. Caporini, D. Lee, S. Hediger, R. G. Griffin, G. De Paëpe, *Chem. Sci.* **2017**, *8*, 8150–8163.
- [113] S. Hediger, D. Lee, F. Mentink-Vigier, G. De Paëpe, *eMagRes*, **2018**, *7*, 105–116.
- [114] P. Gast, D. Mance, E. Zurlo, K. L. Ivanov, M. Baldus, M. Huber, *Phys. Chem. Chem. Phys.* **2017**, *19*, 3777–3781.
- [115] R. Harrabi, T. Halbritter, F. Aussenac, O. Dakhlaoui, J. Van Tol, K. K. Damodaran, D. Lee, S. Paul, S. Hediger, F. Mentink-Vigier, S. T.h. Sigurdsson, G. De Paëpe, *Angew. Chem. Int. Ed.* **2022**, *61*, e202114103.
- [116] L. Niccoli, G. Casano, G. Menzildjian, M. Yulikov, T. Robinson, S.-E. Akrial, Z. Wang, C. Reiter, A. Porea, D. Siri, A. Venkatesh, L. Emsley, D. Gajan, M. Lelli, O. Ouari, A. Lesage, *Chem. Sci.* **2024**, 16582–16593.
- [117] C. Ysacco, E. Rizzato, M.-A. Virolleaud, H. Karoui, A. Rockenbauer, F. Le Moigne, D. Siri, O. Ouari, R. G. Griffin, P. Tordo, *Phys. Chem. Chem. Phys.* **2010**, *12*, 5841.
- [118] F. A. Perras, A. Sadow, M. Pruski, *ChemPhysChem* **2017**, *18*, 2279–2287.
- [119] J. Soetbeer, P. Gast, J. J. Walsh, Y. Zhao, C. George, C. Yang, T. M. Swager, R. G. Griffin, G. Mathies, *Phys. Chem. Chem. Phys.* **2018**, *20*, 25506–25517.
- [120] F. Mentink-Vigier, T. Dubroca, J. Van Tol, S. T. Sigurdsson, *J. Magn. Reson.* **2021**, *329*, 107026.
- [121] C. Sauvée, G. Casano, S. Abel, A. Rockenbauer, D. Akhmetzyanov, H. Karoui, D. Siri, F. Aussenac, W. Maas, R. T. Weber, T. Prisner, M. Rosay, P. Tordo, O. Ouari, *Chem. - Eur. J.* **2016**, *22*, 5598–5606.
- [122] S. S. Eaton, G. R. Eaton, *eMagRes*, **2016**, *5* 1543–1556.
- [123] W. Zhai, A. Lucini Paioni, X. Cai, S. Narasimhan, J. Medeiros-Silva, W. Zhang, A. Rockenbauer, M. Weingarth, Y. Song, M. Baldus, Y. Liu, *J. Phys. Chem. B* **2020**, *124*, 9047–9060.
- [124] X. Cai, A. Lucini Paioni, A. Adler, R. Yao, W. Zhang, D. Beriashvili, A. Safeer, A. Gurinov, A. Rockenbauer, Y. Song, M. Baldus, Y. Liu, *Chem. - Eur. J.* **2021**, *27*, 12758–12762.
- [125] R. Yao, D. Beriashvili, W. Zhang, S. Li, A. Safeer, A. Gurinov, A. Rockenbauer, Y. Yang, Y. Song, M. Baldus, Y. Liu, *Chem. Sci.* **2022**, *13*, 14157–14164.
- [126] T. Halbritter, R. Harrabi, S. Paul, J. Van Tol, D. Lee, S. Hediger, S. T.h. Sigurdsson, F. Mentink-Vigier, G. De Paëpe, *Chem. Sci.* **2023**, *14*, 3852–3864.
- [127] S. R. Chaudhari, P. Berruyer, D. Gajan, C. Reiter, F. Engelke, D. L. Silverio, C. Copéret, M. Lelli, A. Lesage, L. Emsley, *Phys. Chem. Chem. Phys.* **2016**, *18*, 10616–10622.
- [128] D. J. Kubicki, A. J. Rossini, A. Porea, A. Zagdoun, O. Ouari, P. Tordo, F. Engelke, A. Lesage, L. Emsley, *J. Am. Chem. Soc.* **2014**, *136*, 15711–15718.
- [129] M. Rosay, PhD thesis, Massachusetts Institute of Technology **2001**.
- [130] A. Leavesley, C. B. Wilson, M. Sherwin, S. Han, *Phys. Chem. Chem. Phys.* **2018**, *20*, 9897–9903.
- [131] D. A. Hall, D. C. Maus, G. J. Gerfen, S. J. Inati, L. R. Becerra, F. W. Dahlquist, R. G. Griffin, *Science* **1997**, *276*, 930–932.
- [132] Ü. Akbey, W. T. Franks, A. Linden, S. Lange, R. G. Griffin, B.-J. van Rossum, H. Oschkinat, *Angew. Chem. Int. Ed.* **2010**, *49*, 7803–7806.
- [133] C. Sauvée, M. Rosay, G. Casano, F. Aussenac, R. T. Weber, O. Ouari, P. Tordo, *Angew. Chem. Int. Ed.* **2013**, *52*, 10858–10861.
- [134] I. Marin-Montesinos, J. C. Paniagua, M. Vilaseca, A. Urtizberea, F. Luis, M. Feliz, F. Lin, S. Van Doorslaer, M. Pons, *Phys. Chem. Chem. Phys.* **2015**, *17*, 5785–5794.
- [135] E. L. Dane, T. Maly, G. T. Debelouchina, R. G. Griffin, T. M. Swager, *Org. Lett.* **2009**, *11*, 1871–1874.
- [136] E. L. Dane, T. M. Swager, *J. Org. Chem.* **2010**, *75*, 3533–3536.
- [137] O. Haze, B. Corzilius, A. A. Smith, R. G. Griffin, T. M. Swager, *J. Am. Chem. Soc.* **2012**, *134*, 14287–14290.
- [138] S. Mandal, S. T. Sigurdsson, *Chem. Commun.* **2020**, *56*, 13121–13124.
- [139] K.-N. Hu, V. S. Bajaj, M. Rosay, R. G. Griffin, *J. Chem. Phys.* **2007**, *126*, 044512.
- [140] Y. Liu, F. A. Villamena, A. Rockenbauer, Y. Song, J. L. Zweier, *J. Am. Chem. Soc.* **2013**, *135*, 2350–2356.
- [141] S. Bothe, J. Nowag, V. Klimavičius, M. Hoffmann, T. I. Troitskaya, E. V. Amosov, V. M. Tormyshev, I. Kirilyuk, A. Taratayko, A. Kuzhelev, D. Parkhomenko, E. Bagryanskaya, T. Gutmann, G. Buntkowsky, *J. Phys. Chem. C* **2018**, *122*, 11422–11432.
- [142] K. Sato, R. Hirao, I. Timofeev, O. Krumkacheva, E. Zaytseva, O. Rogozhnikova, V. M. Tormyshev, D. Trukhin, E. Bagryanskaya, T. Gutmann, V. Klimavicius, G. Buntkowsky, K. Sugisaki, S. Nakazawa, H. Matsuoka, K. Toyota, D. Shiomi, T. Takui, *J. Phys. Chem. A* **2019**, *123*, 7507–7517.
- [143] J. A. Meckes, Z. W. Schroeder, D. Sarkar, R. W. Hooper, C. E. Faraday-Smith, A. Brown, R. R. Tykwinski, V. K. Michaelis, *J. Am. Chem. Soc.* **2025**.
- [144] C. Reichardt, T. Welton, in *Solvents and Solvent Effects in Organic Chemistry*, 4 ed., Wiley-VCH Verlag GmbH & Co. KGaA, **2010**, pp. 7–64.
- [145] W. Moore, R. Yao, Y. Liu, S. S. Eaton, G. R. Eaton, *J. Magn. Reson.* **2021**, *332*, 107078.
- [146] F. J. Scott, T. Dubroca, R. W. Schurko, S. Hill, J. R. Long, F. Mentink-Vigier, *J. Magn. Reson.* **2024**, *365*, 107742.
- [147] D. G. Mitchell, R. W. Quine, M. Tseitlin, R. T. Weber, V. Meyer, A. Avery, S. S. Eaton, G. R. Eaton, *J. Phys. Chem. B* **2011**, *115*, 7986–7990.
- [148] V. K. Michaelis, A. A. Smith, B. Corzilius, O. Haze, T. M. Swager, R. G. Griffin, *J. Am. Chem. Soc.* **2013**, *135*, 2935–2938.
- [149] M. Rosay, M. Blank, F. Engelke, *J. Magn. Reson.* **2016**, *264*, 88–98.
- [150] T. F. Kemp, H. R. W. Dannatt, N. S. Barrow, A. Watts, S. P. Brown, M. E. Newton, R. Dupree, *J. Magn. Reson.* **2016**, *265*, 77–82.
- [151] I. V. Sergeev, F. Aussenac, A. Porea, C. Reiter, E. Bryerton, S. Retzlöff, J. Hesler, L. Tometich, M. Rosay, *Solid State Nucl. Magn. Reson.* **2019**, *100*, 63–69.

Manuscript received: March 14, 2025

Revised manuscript received: May 22, 2025

Manuscript accepted: May 26, 2025

Version of record online: June 02, 2025